Part 1

Introduction

1 Biomedical Applications of Nanomaterials: An Overview

Sunil K. Singh, Paresh P. Kulkarni, Debabrata Dash

Banaras Hindu University, Varanasi, India

1.1 Introduction

Nanotechnology (the Greek word *nano* means "dwarf") is the creation and utilization of materials, devices, and systems through the control of matter at the nanometer-length scale, i.e., at the level of atoms, molecules, and supramolecular structures. It is the popular term for the construction and utilization of functional structures with at least one characteristic dimension measured at nanometer scale – a nanometer (nm) is one-billionth of a meter (10^{-9} m). This is roughly four times the diameter of an individual atom. The width of DNA is approximately 2.5 nm and protein molecules measure 1–20 nm. It is essential to understand nanomaterials and their properties in order to develop innovations in biological systems and medicine. However, it is only in the last 5 years that a new branch of science, known as "*nanomedicine*," has emerged as a distinct field, and it has since grown exponentially. The late Nobel physicist Richard P. Feynman had the visionary idea that tiny nanorobots could be designed, manufactured, and introduced into the human body to perform cellular repairs at the molecular level. In his prescient 1959 talk, "There's plenty of room at the bottom," he proposed using machine tools to make smaller machine tools, which could be used in turn to make still smaller machine tools, and so on all the way down to the atomic level [1]. Feynman was clearly aware of the potential medical applications of the new technology he was proposing. As perceived by Feynman, it is extremely likely that nanomedicine, a multidisciplinary field that embraces biology, chemistry, physics, engineering, and materials science, will play a major role in the betterment of the human condition.

Nanomedicine offers examples of how nanotechnological tools are being utilized in biomedical research. The overall goal of nanomedicine is the same as it always has been in medicine: to diagnose as accurately and early as possible, to treat as effectively as possible without side effects, and to evaluate the efficacy of treatment noninvasively. The promise that nanotechnology brings is multifaceted, offering not only improvements to current techniques but also providing entirely new tools and capabilities. By manipulating drugs and other

Bio-Nanotechnology: A Revolution in Food, Biomedical and Health Sciences, First Edition. Edited by Debasis Bagchi, Manashi Bagchi, Hiroyoshi Moriyama, and Fereidoon Shahidi.

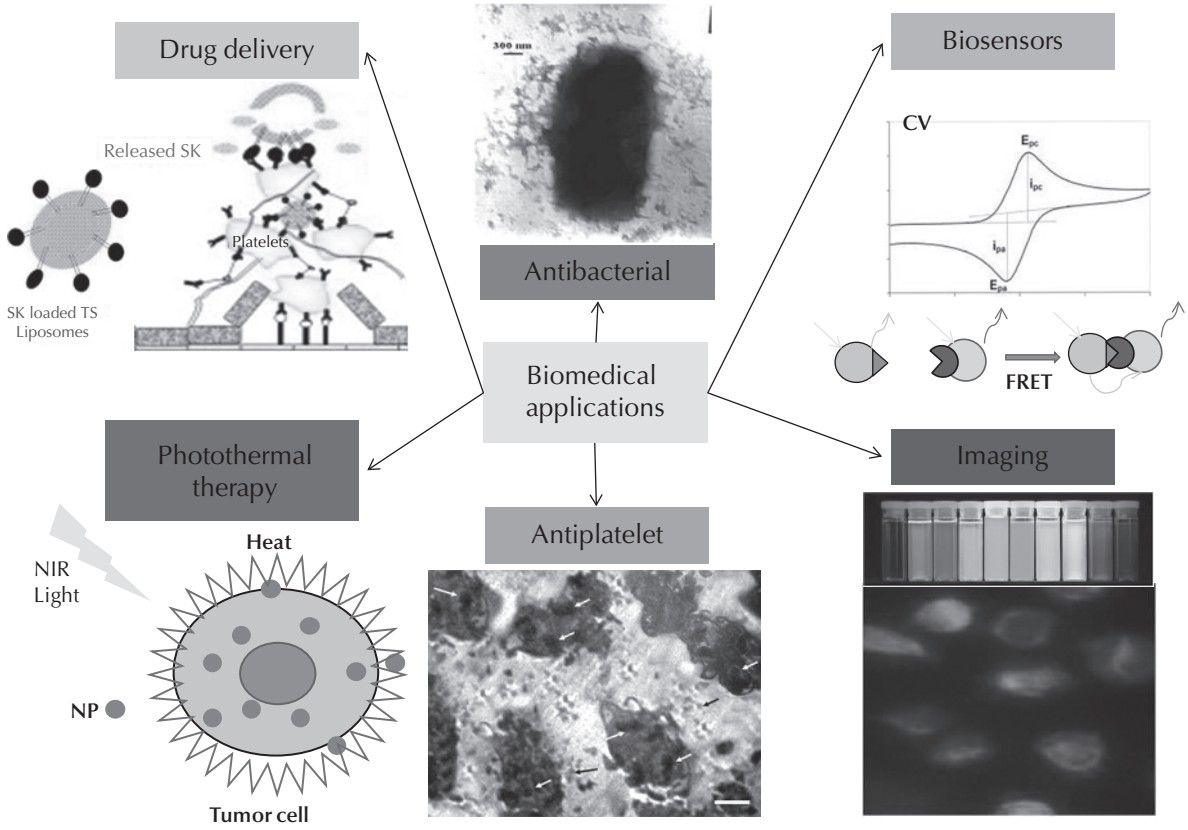

Fig. 1.1 Biomedical applications of nanoparticles. (For a colour version of this figure, please refer to colour plate section 1.)

materials at the nanometer scale, their fundamental properties and bioactivity can be altered. These tools can permit control over characteristics of drugs or agents such as solubility, blood pool retention times, controlled release over short or long durations, environmentally triggered controlled release, or highly specific site-targeted delivery. Furthermore, by using nanometer-sized particles, the increased functional surface area per unit volume can be exploited in various ways. This chapter presents some of the more recent successes in applying various nanomaterials and tools in the biomedical field. It also gives researchers a comprehensive overview of the present status and suggests future directions for employing nanomaterials to attain as yet unmet biomedical goals.

The unique optical, magnetic and electronic properties of nanomaterials provide promising platforms for a wide variety of biomedical applications [2–8] including biosensing, imaging, and drug delivery (see Fig. 1.1). As all the properties of nanomaterials are size- and shape-dependent, the study of methods for their preparation is one of the primary research areas. Traditionally, synthetic approaches to nanomaterials have been divided into two categories: "top-down" and "bottom-up." A typical "top-down" procedure – also called a physical method – involves the mechanical grinding of bulk material and the subsequent stabilization of the resulting nanosized particles by the addition of colloidal protecting agents [9–10]. A "bottom-up" procedure attempts to build nanomaterials and devices one molecule/atom at a time, much in the same way that living organisms synthesize macromolecules. In this chapter we provide an overview of synthetic approaches to carbon-based nanomaterials, wet chemical methods for the fabrication of metallic nanoparticles (NPs) that

rely on the chemical reduction of metal salts, and biocompatible synthesis procedures for quantum dots and other biomedically important nanomaterials. A large variety of stabilizers such as donor ligands and surfactants, as well as surface modifications or functionalization, are used to control the growth of the primarily formed nanoclusters and to prevent them from agglomerating [11–16]. Depending upon the nature of the materials and their unique properties, nanomaterials can be categorized as follows.

- **Metallic NPs:** Among the different nanomaterials employed in biomedical research, metallic NPs have proved to be the most convenient and suitable. Based on their unique optical, physical, and electrical properties, metallic NPs have found significant applications in a wide spectrum of biomedical utilities such as imaging, sensing, drug delivery, and gene targeting [17–22]. Reports from our laboratory and others suggest that some of these NPs also have significant therapeutic potential [23–38]. Their applications are constantly increasing in view of the relatively lesser toxicity reported with these NPs. In the second section of this chapter we discuss biomedically important and extensively studied metallic NPs such as silver and gold nanoparticles.
- **Carbon-based nanomaterials:** Carbon nanomaterials (CNs) include fullerenes, nanotubes, nanodiamonds (ND), and graphene.
- **Fullerenes:** Fullerenes are novel carbon allotropes with a polygonal structure made up exclusively of 60 carbon atoms. Soluble derivatives of fullerenes such as C60, with a soccer ball–shaped arrangement of 60 carbon atoms per molecule, show great promise as pharmaceutical agents. Nanostructures are characterized by the presence of numerous points of attachment whose surfaces can be functionalized for tissue binding. These derivatives, many of which are already in clinical trials, have good biocompatibility and exhibit low toxicity even at relatively high dosages. Fullerene compounds can be employed as antiviral agents, most notably against human immunodeficiency virus [39], antibacterial agents (e.g., *Escherichia coli* [40], *Streptococcus* [41], *Mycobacterium tuberculosis* [42]), photodynamic agents for anticancer therapy [43–45], antioxidant and antiapoptotic agents for the treatment of amyotrophic lateral sclerosis [46] and Parkinson's disease [47], and in many other applications.
- **Carbon nanotubes** (CNTs)**:** CNTs are one of the most widely used nanomaterials because of their remarkable physical, chemical, and biological properties. There are two classes of CNTs: single-walled (SWCNTs) and multiwalled (MWCNTs). Theoretically, nanotubes are viewed as rolled-up structures of single or multiple sheets of graphene to give SWCNTs and MWCNTs, respectively. These one-dimensional carbon allotropes have a large surface area, high mechanical strength with ultra-light weight, rich electronic properties, and excellent chemical and thermal stability. Because of their unique physiochemical properties, researchers have been exploring their potential in biological and biomedical applications [48–54]. CNTs can easily be surface functionalized to bind proteins and nucleic acids, and hence are emerging as novel components in nanoformulations for the delivery of therapeutic molecules [5, 55].
- **Nanodiamond particles (NDP):** Diamond NPs have been investigated as single-particle biomarkers for fluorescence imaging [56–58]. The surface of NDP can be functionalized to bind proteins and nucleic acids, allowing NDP to be used as a carrier for pharmaceutical agents or oligonucleotides [59–62].
- **Graphene:** The distinct structural properties of graphene, in particular its high aspect ratio, propensity to functional modification, unique electronic and optical properties, as well as its potential biocompatibility, makes it an extremely attractive candidate for biomedical applications such as biosensor development, imaging, drug delivery, bacterial inhibition, and photothermal therapy [16, 63–72].
- **Quantum dots** (QDs)**:** QDs are semiconductor nanocrystals with spatially confined excitation states. Crucial for their biological applications is the need to coat them with other materials to allow their aqueous dispersion and to prevent leakage of the toxic heavy metals. QDs have been widely used in imaging and cell labeling either *in vitro* or *in vivo* [73–75]. QDs have also been successfully used to quantify fluorescence

in *in situ* hybridization signals [76, 77], as well as in charge transfer–based biosensors [78], drug delivery [79], and photodynamic therapy [80].

- **Other biomedically important nanomaterials:** Apart from the nanomaterials discussed above, various other nanoparticles have widespread acceptance in the biomedical field, including magnetic nanoparticles, which provide many exciting opportunities in biomedical applications. The ease of optimization of size according to requirement, manipulability by external magnetic force, contrast enhancement in magnetic resonance imaging (MRI), and other such desirable properties of magnetic NPs have recently been exploited in various applications in the field of biology and medicine, including protein purification, drug delivery, imaging, tagging, sensing, and separation [81, 82].
- **Polymeric nanoparticles** are colloidal structures composed of synthetic or semisynthetic polymers. Polymers such as polysaccharide chitosan–polylactic acid, polylactic acid coglycolic acid, poly-caprolactone, and chitosan nanoparticles have been used as drug carriers [83–85]. The drug is dissolved, entrapped, encapsulated, or attached to a nanoparticle matrix.
- **Liposomes** are nanoparticles comprising a lipid bilayer membrane surrounding an aqueous interior. The amphiphilic molecules used for the preparation of these molecules have similarities between the biologic membranes and so have been used for improving the efficacy and safety of new drugs [86–88].
- **Solid lipid nanoparticles** have been proposed as a new type of colloidal drug carrier system suitable for intravenous administration [89]. The system consists of spherical solid lipid particles in the nanometer range, which are dispersed in water or in surfactant solution.

1.2 Metallic NPs

Among the different nanomaterials used in biomedical research, metallic NPs have proven to be the most convenient and suitable. The properties of NPs depend on their structure and composition, and can typically be engineered or modified by changing the relative influence of interfacial properties and bulk properties through the characteristic dimensions of the components. The principal parameters of NPs are their shape, size, and the morphological substructure.

As most properties of metallic NPs are size- and shape-dependent, methods for their preparation are one of the primary areas of interest for nanoscientists. Nanostructured metal colloids could be obtained by "top-down" and "bottom-up" approaches as discussed in Introduction section. Synthesis of biocompatible or biogenic NPs is one of the major challenges to be overcome so as to realize their biomedical application. In this context, some major advances have been made by employing methods based on chemical reactions in solution (often termed "wet chemistry"). A wet chemical procedure involves growing nanoparticles in a liquid medium containing various reactants, in particular reducing agents such as sodium borohydride [29], potassium bitartrate [90], methoxypolyethylene glycol [91], or hydrazine [92]. However, in most of these procedures the strong chemical reductants have now been replaced by more biocompatible reagents such as glucose. Stabilizing agents such as donor ligands, polymers, and surfactants are often employed to prevent NPs from agglomerating and to make them easily miscible under cellular conditions. A surfactant is a molecule that is dynamically adsorbed to the surface of the NPs under the reaction conditions. It must be mobile enough to provide access for the addition of monomer units, while remaining stable enough to prevent the aggregation of NPs. Some examples of suitable surfactants or stabilizing agents include alkyl thiols, phosphines, phosphine oxides, phosphates, amides or amines, carboxylic acids, sodium dodecyl benzyl sulfate, or polyvinyl pyrrolidone [12, 13, 92]. As most of the surfactants used have low compatibility with cells and tissues, bovine serum albumin is a popular choice for use as a stabilizing agent. Scientists have recently endeavored to make use of microorganisms as possible eco-friendly nanofactories for the synthesis of metallic NPs [93] such as cadmium sulfide [94], gold [95], and silver [96]. In recent years, metallic NPs and their alloys have been studied extensively in various fields such as sensor technology [18], optical devices [3], catalysis [97], biological labeling [98], drug delivery systems [21], and

treatment of some cancers [99]. Metallic NPs are suitable as markers for the optical detection of biomolecules due to their excellent SPR (surface plasmon resonance) properties. Reports from our laboratory and others suggest that some of these NPs can also have significant therapeutic potential as antimicrobial [24, 29] and antiplatelet agents [23] as well as for the stabilization of proteins, drug delivery, and photothermal tumor ablation. These are extremely promising prospects in the field of health and medicine. Here we discuss the biomedical applications of two extensively exploited metallic NPs: silver and gold.

1.2.1 Silver NPs and their biomedical applications

Nanosilver particles are generally smaller than 100 nm and contain 20–15,000 silver atoms (see Fig. 1.2). Silver NPs (AgNPs) have been receiving considerable attention as a result of their unique physical, chemical, and biological properties, and have found important applications in optics, electronics, and medicine. In addition, nanosilver has innate antimicrobial [24, 29] and antiparasitic activity [100]. Silver NPs support surface plasmons, attributed to the collective oscillation of electrons on the particle surface upon excitation with electromagnetic radiation, which contributes to their unique optical properties. At specific wavelengths of light, the surface plasmons are driven into resonance and the AgNPs have a distinct color that is a function of their size, shape, and environment. The plasmon resonance of silver NPs is responsible for the yellow color of the solution. Any visible change in the color of NPs in solution typically indicates a change in the extent of aggregation of these NPs. The peak absorption wavelength of AgNPs is in the range of 405–430 nm and is evidence for the formation of AgNPs.

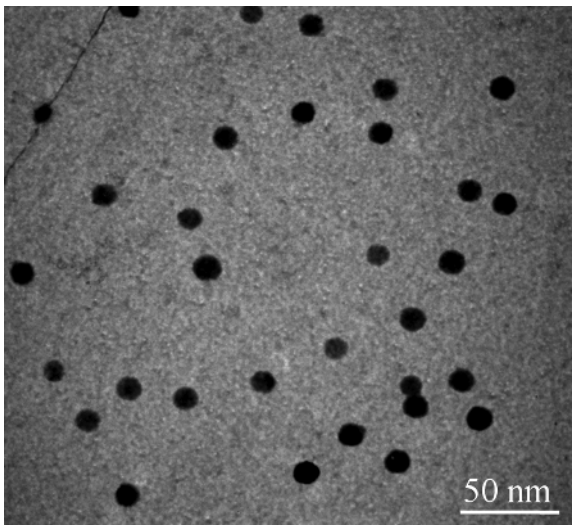

Fig. 1.2 Transmission electron micrograph showing silver nanoparticles.

As described in previous reports, we have successfully synthesized biocompatible AgNPs with enhanced stability and significant antibacterial activity by using glucose as the reducing agent [24] and bovine serum albumin as the stabilizing agent [101]. As mentioned above, another approach to the synthesis of biocompatible silver NPs that is a biogenic process involves the utilization of microorganisms. Several attempts have been made in this direction. When the bacterium *Pseudomonas stutzeri* AG259, isolated from a silver mine, is placed in a concentrated aqueous solution of silver nitrate, it brings about reduction of Ag^+ ions and the formation of AgNPs of well-defined size and distinct topography within its periplasmic space [102]. Ahmad *et al*. (2003) and Nanda and Saravanan (2009) have also successfully synthesized silver NPs using the fungus *Fusarium oxysporum* [96] and the bacterium *Staphylococcus aureus* [103], respectively. Based on their unique physiochemical properties, AgNPs have found significant applications in a wide spectrum of biomedical utilities such as imaging and therapeutics, especially as antimicrobial agents.

1.2.1.1 Antimicrobial properties

Silver nanoparticles have been shown to exhibit significant antimicrobial activity as well as enhancing the action of conventional antibiotics [104]. They have cidal activity against several bacterial species, and are in fact more efficient and broad-spectrum than the majority of conventional antibiotics. Recent studies have also shown that nanosilver has higher microbicidal activity than ionic silver. The study demonstrated the ability of colloidal silver to inhibit the growth and multiplication of

bacterial strains including those that are multi-drug resistant. The antimicrobial activity of colloidal silver particles is influenced by the dimensions as well as the shape of the particles; the bactericidal activity increasing with a decrease in size of the particles. Recently one group has successfully synthesized AgNPs having broad-spectrum activity with efficacy against both Gram-positive and Gram-negative bacteria [104]. Thus, NPs of silver have extensively been investigated for their antibacterial properties. Considerable efforts have been made to explore this activity through electron microscopy, which has revealed a size-dependent interaction of AgNPs with bacteria [105]. The study concluded that nanosilver particles mainly in the size range of 1–10 nm attach to and disrupt the cell membrane. They were also found distributed within the cell, affecting other important cell organelles. NPs of silver have been used as a medium for antibiotic delivery, and to synthesize composites for use as disinfecting filter and coating materials [32]. However, the bactericidal properties of these NPs depend on their stability in the growth medium, since this provides a greater retention time for bacterium–nanoparticle interaction. It has proved challenging to prepare NPs of silver stable enough to significantly restrict bacterial growth. In our earlier report [24], we demonstrated the synthesis of highly stable NPs of silver endowed with significant antibacterial properties (see Fig. 1.3).

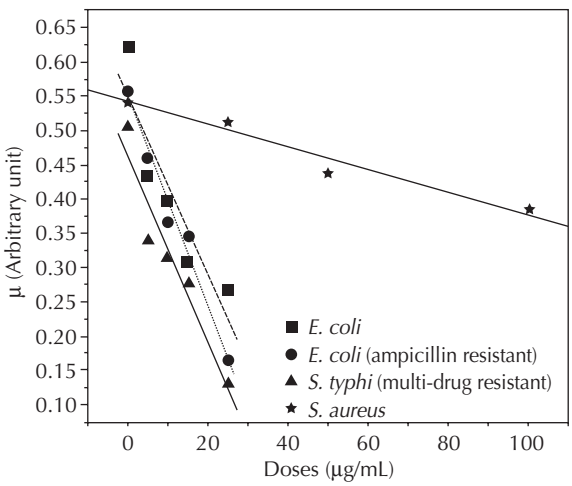

Fig. 1.3 Dose-dependent inhibition of growth rate (μ) of different bacterial strains by silver nanoparticles.

Efforts have been made to understand the underlying molecular mechanism of such antimicrobial actions. In this report we have for the first time shown that silver NPs can change the protein profile of bacteria by interacting with protein molecules that are involved in bacterial cell signaling. Bactericidal properties of the NPs are related not only to the direct effects of silver NPs accumulating intracellularly or at the cell membrane, but also to the ionic or dissolved silver derived from NPs, which also possesses significant antibacterial properties.

In addition, NPs of silver also exhibit antiviral and antifungal properties. It has been reported by Elechiguerra *et al*. (2005) that AgNPs in the size range 1–10 nM bind with HIV-I in a size-dependent fashion [26]. These authors have shown that silver NPs inhibit HIV-1 infection in $CD4^+$ MT-2 cells and cMAGI HIV-1 reporter cells. Kim *et al*. evaluated the efficacy of AgNPs as an antifungal agent against yeast [29].

1.2.1.2 Bio-imaging

Due to good surface characteristics, ease of preparation, and easily accessible excitation wavelengths in the visible range, silver is the most preferred metallic substrate for surface enhanced Raman spectroscopy (SERS). SERS is a powerful and sensitive analytical tool for the detection and identification of a wide range of molecules and is even suitable for single molecule detection. Due to its high sensitivity and the fact that water has very weak Raman scattering, SERS has been recognized as one of the most effective tools for biomolecule detection. Aqueous solutions of AgNPs have been extensively used for identifying proteins, studying the interactions of various drugs with proteins for drug discovery, understanding the effects of pH and other factors on the conformation of proteins, for DNA detection at concentrations down to 10^{-13} M, for developing microarray type gene probes, and for biodetection and biolabeling. Novel fabrication techniques to develop unique nanostructured silver-based SERS substrates to fully exploit the tremendous potential of SERS in biomedical research are currently ongoing. Metal-enhanced fluorescence (MEF) is the increase in fluorescence emission intensity of fluorescent molecules when placed near metallic NPs. The

quantum yield, excitation rate, and photostability of weakly fluorescing species can be significantly increased by silver nanoparticles. Therefore, MEF could considerably improve the performance of current fluorescence-based techniques by using silver NP-coated substrates and could make a significant impact in areas such as drug discovery, high throughput screening, immunoassays, clinical diagnostics, and protein–protein detection. Aptamer-based silver nanoparticles are used in intracellular protein imaging and single NP spectral analysis, where the AgNPs act as an illumiophore and the aptamer as a biomolecule-specific recognition unit [106].

1.2.1.3 Therapeutics

Nanosilver is also used as a biocide to prevent infection in burns, traumatic wounds, and diabetic ulcers [37]. Other uses include improved surface coating for indwelling catheters and other medical devices implanted on/within the body [38]. Tian *et al*. investigated the effect of AgNPs on wound healing and scar tissue formation using thermal injury, diabetic wound, and chronic wound models in mice [107]. This study also demonstrated the efficacy of AgNPs in controlling local and systemic inflammatory responses following burn injury by cytokine modulation. Recently, we have for the first time shown that nanosilver has innate antiplatelet properties and that it effectively prevents integrin-mediated platelet responses, both *in vivo* and *in vitro*, in a concentration-dependent manner (see Fig. 1.4) [23]. Our findings further suggest that these NPs do not possess any lytic activity against platelets and hold the potential to be promoted as antiplatelet/antithrombotic agents after a careful evaluation of toxic effects. Thus, nanosilver is expected to have increasing applications in medicine and related disciplines.

1.2.2 Gold nanoparticles and their biomedical applications

In past decades, gold NPs (AuNPs) have aroused considerable interest and have been explored as a model platform for biomedical research because of their unique physical and chemical properties [4, 17,108, 109]. Gold particles are inert, which makes them relatively more biocompatible. The synthesis of AuNPs with diameters ranging from a few to several hundred nanometers is well established in aqueous solution as well as in organic solvents. Like AgNPs, AuNPs are synthesized through a chemical reduction method. In a typical synthesis, gold salts such as $HAuCl_4$ are reduced by the addition of a reducing agent that leads to the nucleation of Au ions to NPs. Turkevich *et al*. (1951) for the first time synthesized the colloidal gold Au^0 from Au^{III} by using citric acid as the reducing agent [110], a method that is still used nowadays after subsequently replacing the citrate ligand of these AuNPs with the appropriate ligands of biological interest [19]. Recent modifications of the Turkevich method have allowed better size distribution and size control within the 9–120 nm range [111]. In addition, stabilizing agents are also required, which are either adsorbed or chemically bound to the surface of the AuNPs. These agents (also known as surfactants) are typically charged, so that like-charged NPs repel each other, rendering them colloidally stable. Although AuNPs can be stabilized by a large variety of stabilizers (ligands, surfactants, polymers, dendrimers, biomolecules, etc.), the most robust AuNPs, discovered by Giersig and Mulvaney (1993), were stabilized by thiolates using the strong Au–S bond between the soft acid Au and the soft thiolate base [112]. Along these lines, by far the most popular synthetic method using such sulfur coordination for AuNP stabilization is the Shiffrin–Brust biphasic synthesis using $HAuCl_4$, a thiol, tetraoctylammonium bromide, and $NaBH_4$ in water–toluene, yielding thiolate-AuNPs [113]. Since the solubility of these AuNPs is controlled by the solubilizing properties of the terminal group of the thiolate ligands, AuNPs can be transferred from an aqueous phase to an organic phase or *vice versa* by appropriate ligand exchange.

Water-soluble AuNPs typically contain terminal carboxylate groups at their periphery. The carboxyl group is used to attach to the amino groups of biomolecules using 1-ethyl-3(3-dimethylaminopropyl)-carbodiimide-HCl (EDC) [114]. With related strategies almost all kinds of biological molecules can be attached to the particle surface. Although such protocols are relatively well established, bioconjugation of Au nanoparticles is still not trivial and characterization of the synthesized conjugates is necessary, in particular

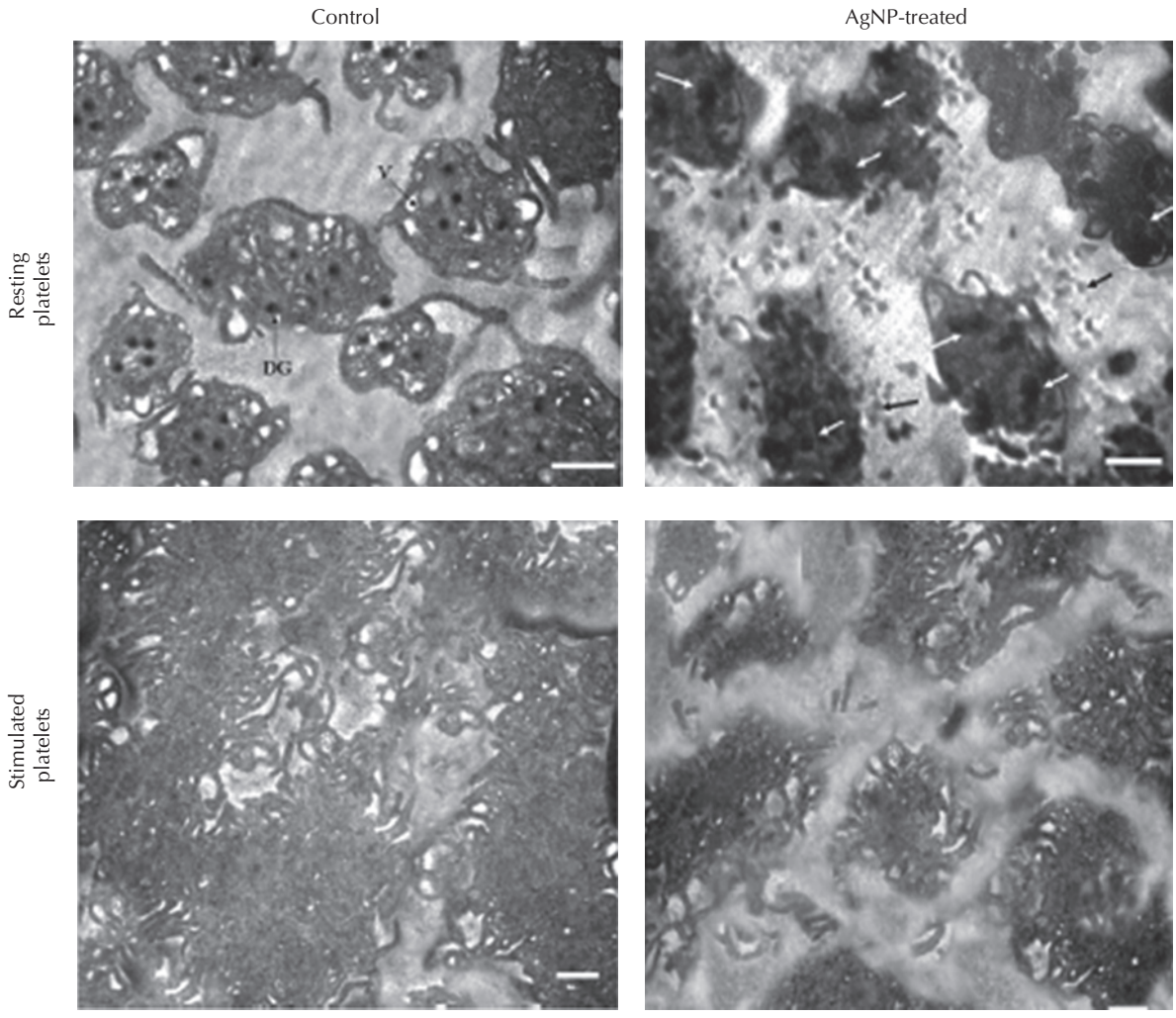

Fig. 1.4 Transmission electron micrographs demonstrating inhibition of platelet activation by silver nanoparticles.

to rule out aggregation effects or non-specific binding during the conjugation reaction. In particular, the number of attached molecules per gold nanoparticle is only a rough estimate in many conjugation protocols, as no standard method for determining the surface coverage of particles modified with molecules has yet been established [115]. Interestingly, it is possible to synthesize not only spherical AuNPs but also other geometries such as rod-shaped particles or hollow shells by using the appropriate techniques. Au nanoparticles have been primarily used for labeling applications. In this regard, the particles are directed and enriched at the region of interest and provide contrast for the observation and visualization of this region.

Gold particles strongly absorb and scatter visible light. Upon absorption, the light energy excites the free electrons in Au particles to a collective oscillation, the so-called surface Plasmon resonance (SPR). Generally, the optical properties of small metal NPs are dominated by SPR [19, 116, 117]. For gold, it happens that the resonance frequency is governed by its bulk dielectric constant and lies in the visible region of the electromagnetic spectrum

[117]. Because NPs have a high surface area to volume ratio, the plasmon frequency is exquisitely sensitive to the dielectric (refractive index) nature of its interface with the local medium. Any change in the environment of these particles (surface modification, aggregation, medium refractive index, etc.) leads to colorimetric changes in the dispersions [19, 118]. Due to coupling of the plasmons, assemblies (or aggregations) of AuNPs are often accompanied by distinct color changes from red (dispersed) to blue (aggregated). AuNPs have optical, electronic, catalytic, and biocompatible properties and potentially high surface reactivity compared with other metallic NPs.

1.2.2.1 Bio-imaging

AuNPs are a very attractive contrast agent as they can be visualized using a variety of techniques. The most usual detection techniques are based on the interaction between AuNPs and light. The absorption and scattering of electromagnetic radiation by noble metal NPs are strongly enhanced. These unique properties provide the potential for designing novel optically active reagents for molecular imaging. In *in vitro* studies, gold nanorods act as novel contrast agents for molecular imaging [119]. Two-photon luminescence imaging of cancer cells has been achieved using gold nanorods. They have also been reported to be valuable for cell imaging using techniques such as dark field light SPR scattering. The use of near-infrared (NIR)-absorbing gold nanoparticles can significantly enhance the image contrast due to the more substantial differences in optical absorption than the endogenous tissue chromophores. Gold NPs are also used in *in vivo* imaging.

Beyond the applications for visible light imaging, Au particles also provide excellent contrast for TEM (transmission electron microscopy) imaging with high lateral resolution. Unlike fluorescence labeling, contrast enhancement in TEM using Au particles is more stable, as it does not suffer from photobleaching, which is a major limitation for fluorescence-based methods. In addition, better lateral resolution with high contrast can be obtained with TEM imaging. In immunostaining, molecules/structures are labeled with an excess of Au nanoparticles so that virtually all entities are labeled (possibly with several markers) in order to provide high contrast. AuNPs can be used for single-particle tracking of membrane molecules and also as a contrast agent in X-rays. Like silver NPs, the surface of AuNPs is modified with ligands that can specifically bind the analyte. Upon binding to the Au particle, the Raman signal of the analyte is dramatically enhanced and allows for its detection. Recent developments include AuNPs modified with Raman-active reporter molecules for the detection of DNA or proteins.

1.2.2.2 Therapeutics

AuNPs have long been used for the delivery of molecules into cells. For this purpose the molecules are adsorbed on to the surface of the Au particles and the whole conjugate is introduced into the cells. In gene therapy, DNA is introduced into cells, which subsequently causes the expression of the corresponding proteins. AuNPs have been used to deliver anticancer drugs specifically to cancer tissue. The drug delivery applications do not exploit any special property of gold particles other than the fact that they are small, colloidally stable, relatively easy to conjugate with ligands, and inert, and thus are relatively biocompatible.

In addition, AuNPs can be exploited in cancer treatment based on their photothermal properties. When gold particles absorb light, the free electrons in the gold particles are excited. Excitation at the plasmon resonance frequency causes a collective oscillation of the free electrons. Upon interaction between the electrons and the crystal lattice of the gold particles, the electrons relax and the thermal energy is transferred to the lattice. Subsequently the heat from the gold particles is dissipated into the surrounding environment. Au particles can thus be heated by the absorption of light, whereby the absorbed light energy is converted into thermal energy. Due to the heat generated by the gold particles, the surrounding cancerous tissues can be destroyed locally without exposing the entire organism to elevated temperatures [86–88]. Furthermore, gold nanoshells are sufficiently large (about 100–300 nm in diameter) to have SPR peaks in the NIR region that will provide better tissue penetration. In a pioneering study, human prostate cancer cells incubated with gold nanoshells were found to undergo photothermally induced morbidity upon exposure to NIR light [120].

1.2.2.3 Diagnosis

AuNPs as a class of nanomaterials with many unique properties such as colorimetric conductivity and nonlinear optical properties, have been explored for their potential applications in biomolecular detection. AuNPs can be used to quantitatively detect nucleic acids and proteins in clinical samples. For example, a DNA-based method for rationally assembling gold nanoparticles into macroscopic materials has been reported by Mirkin and co-workers [18, 22, 118]. For protein detection, an aggregation-based immunoassay for antiprotein A using gold nanoparticles has been developed [121]. The hyper-Rayleigh scattering signals of aggregated gold nanoparticles labeled with immunoglobulin G could be used to quantify antibody/antigen in aqueous solution [122]. These two methods could only detect proteins at the microgram level, which limits their applications in immunoassay, especially for early cancer diagnosis. AuNPs can also be used for the transfer of electrons in redox reactions to detect analytes which are substrates to redox enzymes. Due to their small size, gold particle-based sensors could have a significant impact in diagnostics.

1.3 Carbon-based nanomaterials

Carbon nanostructures have been at the forefront of nanoscience for at least 25 years, since the discovery of a novel form of carbon called fullerene in 1985 by Kroto and co-workers [123], which was recognized with a Nobel Prize for Chemistry in 1996. Since then a large family of new carbon materials has been discovered. The most well-known form of fullerene is the buckyball (C60), which is made of 20 hexagons and 12 pentagons of carbon atoms. Almost 6 years later, carbon nanotubes (CNTs), which are considered a new form of fullerenes, were discovered by Sumio Iijima [124]. Thus, only three-dimensional (diamond, graphite), one-dimensional (nanotubes), and zero-dimensional (fullerenes) allotropes of carbon were known. Although the nanocarbon community had grown rapidly due to the addition of fullerene-based researchers, and later CNT-based researchers, graphene *per se* did not attract much interest until the 2004 publication of Novoselov, Geim *et al*. [125], where the authors reported a simple, easily reproducible technique for the preparation of high-quality monolayer and few-layer graphene flakes. Graphene is the name given to a flat monolayer of carbon atoms tightly packed into a two-dimensional (2D) honeycomb lattice. Graphene is the basic building block of other important allotropes; it can be stacked to form 3D graphite, rolled to form 1D nanotubes, and wrapped up to form 0D fullerenes.

In this chapter we briefly discuss the biocompatible synthesis, applications, and toxicity of CNTs and graphene, while further details of these and other carbon-based nanomaterials will be dealt with comprehensively in Chapter 25. Generally, three techniques are being used to produce CNTs: carbon arc-discharge [124], laser-ablation [126], and chemical vapor deposition (CVD) [127]. Novoselov *et al*. [125] first demonstrated the repeatable synthesis of graphene through exfoliation and this is still the most popular technique for graphene synthesis, although efforts are being made to develop new processing routes for the efficient large-scale synthesis of graphene. Generally, the exfoliation can be performed either mechanically or chemically [128]. The primary advantage of chemical exfoliation over the mechanical approach lies in its high-yield and scalability. In general, graphene is synthesized by the Brodie [129], Staudenmaier [130] or Hummers method [131], or some variation of these methods. As the present chapter focuses on the biomedical applications of CNTs and graphene, we do not have room to describe all the existing methods for the preparation of CNTs. Therefore, we discuss here the advances being made to enhance the biocompatibility of CNTs and grapheme, which can then easily be administered under *in vivo* conditions.

For biological and biomedical applications of CNs, it is extremely important for them to be compatible with biological systems, and it is desirable that they should be water-dispersible and nontoxic. Further, there is a growing need to develop biologically benign CNs using nature-friendly synthesis procedures to address the possible environmental concerns about the widespread use of CNs. The recent expansion in methods to chemically

modify and functionalize CNs has made it possible to solubilize and disperse CNs in water, thus opening the pathway for their facile manipulation and processing in physiological environments [132, 133]. In this section, we focus exclusively on methods that have been successfully applied to the modification of CNs with biomolecules. These methods can be divided into three main approaches, depending on the nature of the linkage between biomolecules and CNs, i.e., covalent attachment (chemical bond formation) [133], non-covalent attachment (physical absorption), or a hybrid approach. The most common method, and probably one of the simplest methods of covalent functionalization of CNs, involves reactions with carboxylic acid (–COOH) residues. Biomolecules can be linked to carboxylic acid-functionalized carbon nanotubes and graphene sheets after their activation with *N*-hydroxy succimide (NHS) using standard carbodiimide (EDC) peptide coupling chemistry protocols. The strong non-covalent interactions between CNs and certain aromatic and/or hydrophobic molecules can also be utilized to provide a platform for further functionalization with biomolecules. Polyethylene glycol (PEG) can be used to non-covalently coat carbon nanotubes and prevent non-specific protein absorption [48–55]. These PEG-coated carbon nanotubes can then be further chemically modified to provide sites for chemical or affinity-based linking to proteins. In addition, to make GO (graphene oxide) colloidal solutions more biocompatible and easier to administer under *in vivo* conditions, PEG can also be covalently grafted onto hydroxyl and carboxylic groups of GO with the help of 1,1-carbonyldiimidazole [66, 67]. Hence, PEGylation of CNs could prove to be a valuable tool in improving the biocompatibility of CNs.

All the carbon nanomaterials have very interesting physicochemical properties, such as an ordered structure with high aspect ratio, ultra-light weight, high mechanical strength, high electrical conductivity, high thermal conductivity, metallic or semimetallic behavior, and large surface area. In the last few years, several studies have been proposed, indicating potential applications of CNs [48–72]. Based on their unique optical, physical, and electrical properties, carbon nanostructures have found significant applications in a wide spectrum of biomedical utilities such as sensing, imaging, and therapeutics.

1.3.1 Biosensors

The electronic properties of CNs have been extensively exploited in biosensors. The charge transport properties of CNs make them suitable for application in a variety of biosensors. To understand the potential of CNs in biosensor applications, it is necessary to consider the electronic properties of CNs. The integration of biomolecules with CNs enables the use of such hybrid systems as electrochemical biosensors (enzyme electrodes, immunosensors, or DNA sensors) and active field-effect transistors. The nanometer dimensions of the CNs, together with the unique electronic structure of a graphene sheet, render the electronic properties of these nanostructures highly unusual. The specific advantage of CNTs for integrating biomolecules is their small size, allowing these nanoelectrodes to be plugged into locations where the use of electrochemistry would otherwise be impossible, such as inside proteins [134–136]. One of the opportunities that CNTs will provide is a more efficient way of communicating to the outside world the activity of biological molecules used in biosensors [137]. Typically this communication is achieved via the transfer of electrons. CNT-based sensors have been developed to detect a wide array of biological species including glucose, neurotransmitters, toxins, proteins, and DNA [138, 139]. Several studies have established the utility of graphene-based biosensors using different redox probes such as H_2O_2, NADH, and ascorbic acid [140–144]. Graphene-based biosensors have been employed for sensing several important biomolecules including glucose, DNA, dopamine, and alcohol [63, 64]. In a recent study, cytochrome c was immobilized on a graphene-coated electrode, which was then utilized in the sensing of nitric oxide. This illustrates how a graphene-coated electrode with an antibody or enzyme immobilized on its surface can be utilized in sensing the corresponding antigen or substrate. This substantially widens the possible array of biomolecules that can be detected by graphene-based biosensors. Graphene can also serve as an

excellent candidate for microbial detection and diagnosis [16].

Apart from electrochemical analyzers, biosensors based on the principle of fluorescence resonance energy transfer (FRET) have also utilized GO to detect thrombin, DNA–DNA hybridization, and tumor markers [145–147]. Also, with advances in graphene functionalization and chemical modification techniques, the array of applications for graphene in biosensors is bound to increase dramatically.

1.3.2 Bio-imaging

The intrinsic optical properties of SWNTs and GO make them suitable for use as optical probes. Both SWNTs and GO display optical absorption in the visible as well as the near-infrared (NIR) range. These nanomaterials exhibit strong resonance Raman scattering, high optical absorption, and photoluminescence in the NIR range, all of which have been utilized for imaging in biological systems *in vitro* and *in vivo*. Raman microscopy has been employed to image SWNTs in liver cells, as well as tissue slices [148, 149]. Weisman and co-workers (2007) demonstrated nanotube-based biomedical imaging inside a living animal [150]. In this study, the biodistribution of SWNTs in live *Drosophila* larvae was monitored by the nanotube fluorescence signals through NIR fluorescence microscopy. Recently, a research group successfully used RGD-conjugated PEGylated SWNTs as Raman probes for *in vivo* tumor imaging in live mice [151, 152].

The high optical absorption of SWNTs can also be utilized in photoacoustic imaging, where sound waves are generated as a result of local heating by the absorption of laser light. Photoacoustic imaging has a higher spatial resolution than traditional ultrasound, and deeper tissue penetration than fluorescence imaging [153]. De La Zerda *et al*. used RGD-conjugated SWNTs as the contrast agent for photoacoustic molecular imaging of cancer in a mouse tumor model [154]. This work opens up new opportunities for *in vivo* biological imaging using SWNTs.

Graphene can also be used for cellular imaging based on its unique optical properties. A recent study by Peng *et al*. [66] demonstrated that fluorescein-functionalized PEGylated graphene oxide (GO) exhibits excellent fluorescent properties, and that it can be efficiently taken up by cells and serve as a fluorescent nanoprobe suitable for imaging. Sun *et al*. [7] have shown that GO sheets are photoluminescent in visible and infrared regions, and such intrinsic photoluminescence can be employed for live cell imaging in the near-infrared range without significant background. In a recent study we investigated the intrinsic fluorescence of individual GO sheets using flow cytometry [155]. Upon excitation with a 488 nm laser most of the GO emitted fluorescence in all the three channels in a flow cytometer, with relatively stronger signal in the FL3 channel than in FL1 and FL2. This observation could lead to the effective analysis of graphene–cell interactions using flow cytometry. The inherent optical properties and stable nature of GO suspension promise increasing future applications in the areas of cellular imaging and drug delivery.

1.3.3 Therapeutics

CNs can be excellent tools in drug delivery owing to their small size, large surface to volume ratio, and tendency for non-covalent interaction with drug molecules. CNTs have been extensively investigated as drug carriers. In recent years, different strategies have been developed to conjugate drug molecules to CNTs either through covalent binding or non-covalent adsorption. Covalently bound drug molecules are linked to the functional groups on CNT or to the polymer coating of CNTs. Aromatic drugs with a flat structure can be adsorbed on the surface of CNTs by Π–Π stacking. CNT-based drug carriers have been further utilized for *in vivo* cancer treatment in animal models. CNT–ligand bioconjugates have been widely utilized for cell-specific targeted delivery of drugs in both *in vitro* experiments and some *in vivo* models. Antibody-conjugated PEGylated GO has been shown to be effective in the targeted delivery of anticancer drugs to tumor cells [65, 67]. More importantly, a recent study has shown that potent water-insoluble anticancer drugs could be rendered therapeutically useful by complexing with PEGylated GO [67]. Besides drug delivery, SWNTs and GO can also be utilized as photothermal

therapeutic agents to kill cancer cells [8, 70, 71]. NIR laser irradiation has been used to generate heat, causing the destruction of cancer cells with specific SWNT internalization. Due to strong optical absorption in the NIR range, GO has also been shown to cause photothermal ablation of tumors following intravenous administration in animals. Recent reports have also invested CNTs and GO nanosheets with antibacterial as well as antiparasitic properties [68, 69, 156].

1.4 Quantum dots

Quantum dots (QDs) are near-spherical nanocrystals with a semiconductor core composed of elements from the periodic groups II-VI (CdSe) or III-V (InP), and a shell made of ZnS [157–159]. They have electronic properties intermediate between bulk semiconductors and discrete molecules. Their optical-electronic nature is determined by the size and shape of individual crystals [160, 161]. QDs were first discovered in 1980s by Alexei Ekimov [162], but the term "quantum dot" was coined by Mark Reed. QDs have since found a wide spectrum of applications in transistors, solar cells [163], light emission diodes [164], and diode lasers [165] due to their unique electronic properties. They have also been extensively investigated as agents for biological imaging, and have emerged as a novel class of fluorophores with near ideal characteristics – high quantum yield [166], wide excitation spectra, narrow, tuneable and symmetrical emission spectra [167, 168], and ease of bioconjugation [169]. QDs have also found application in FRET [76, 77] and charge transfer–based biosensors [78], drug delivery [79], and photodynamic therapy [80].

Synthesis procedures for QD have assumed importance due to the size-dependant tenability [160] of their optical properties and the potential toxicity of heavy metals in the core. QDs can be synthesized using a variety of techniques including high-temperature synthesis [170], γ-irradiation [171], microwave-assisted synthesis [172], Langmuir–Blodgett films [173], polyol [174] and sol-gel methods [175]. However, they are typically synthesized by the injection of liquid precursors into hot (300°C) organic solvents, such as TOPO (trioctylphosphine oxide) and hexadecylamine, which serve as ligand molecules [159, 170]. The liquid precursors in earlier reports were extremely toxic and unstable [170], but have since been replaced by less harmful counterparts [159]. The ligands used in the synthesis allow regulation of the nucleation time. This enables synthesis of QDs of different sizes by varying the amount of precursors and crystal growth times [159]. The choice of ligands considerably influences both QD synthesis and the optical properties of synthesized QDs [176]. There are a considerable number of reports where the use of a particular ligand led to the formation of more stable QDs with higher quantum yields [176]. QDs thus synthesized have a heavy-metal semiconductor core made of CdSe, CdS, or CdTe with low quantum yield, typically less than 10%. This has led to the development of type II QDs, also called "core-shell QDs," that consist of a shell of a high band-gap semiconductor, such as ZnS, over the heavy metal core (see Fig. 1.5) [177]. The shell counteracts the defects in the core and dramatically enhances the quantum yield up to 80%. It also confines the hole to the core, protecting the core from oxidation and making them photostable, thus preventing the leaching of heavy metal atoms from the core.

However, these QDs have extremely hydrophobic surfaces and are therefore water-insoluble and unsuitable for biological applications, for which they require surface modification. This is achieved by the replacement of existing ligands with hydrophilic ligands (ligand exchange), or by utilizing the hydrophobic ligands for coating with organic

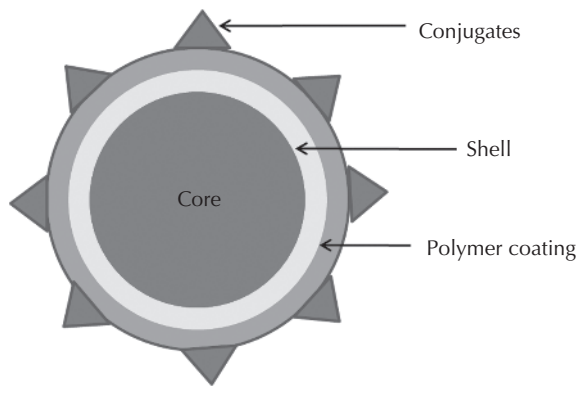

Fig. 1.5 Schematic representation of functionalized core-shell QD. (For a colour version of this figure, please refer to colour plate section 1.)

polymer ligands (ligand capping). One of the most common approaches for surface modification involves the attachment of thiolated PEG polymers [178]. However, such QDs exhibit a low quantum yield. This disadvantage is overcome by using a ligand capping strategy with amphiphilic polymers such as polyacrylic acid [179]. QDs have also been subjected to bio-functionalization by linking them to a variety of biomolecules including streptavidin [180], immunoglobulins [181], oligonucleotides [182], peptides and proteins [183], which enable their use in the labeling of diverse cellular targets.

1.4.1 Properties

By definition, QDs comprise matter whose excitation states are confined in all three spatial dimensions, which is responsible for their unique size-dependent optical and electronic properties. Generally, the smaller the size of a QD, the greater is the energy difference between the highest valence band and the lowest conduction band. Thus, larger QDs, having smaller band gaps, emit light of lower frequency, while smaller QDs emit light of higher frequency (see Fig. 1.6) [184]. Furthermore, due to the small size of the QD nanocrystal, its constituent atoms get excited and emit light simultaneously, leading to high fluorescence intensity. They lack photobleaching due to their inorganic composition, and exhibit a long fluorescence lifetime of 10–40 nanoseconds [161, 180, 181]. Although the theoretical quantum yield of QDs per particle is lower than that of organic fluorophores, their high molar extinction coefficient and long excitation state lifetimes more than compensate, leading to much brighter fluorescence signals than organic dyes. They also exhibit other advantages over fluorophores of a large Stokes shift and extremely high photostability [180]. These characteristics make them near perfect fluorescent markers, superior to organic fluorophores. Since QDs have tuneable, narrow, symmetrical, and bright emission [167, 168], they are particularly useful for multiplex imaging. However, since their brightness is dependent upon their core diameter, the relative brightness of QDs with different emission wavelengths can vary markedly; signal intensity of QDs (size 525 nm) being as much as 17 times and 32 times lower than QDs (size 655 nm) and near-infrared QDs (size 705 nm), respectively [185]. This will have implications for comparisons of expression levels of different elements being detected by multiplex QD imaging, and would require data normalization. Thus, QDs are most suitable for imaging, optical transduction, and photosensitization applications.

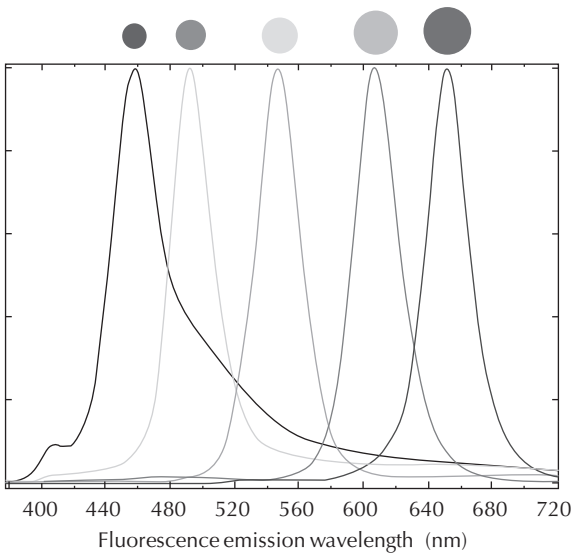

Fig. 1.6 Size-dependence of QD emission spectrum. (For a colour version of this figure, please refer to colour plate section 1.)

1.4.2 Imaging

Since the first report of the use of QDs in immunohistochemistry (IHC) for the detection of actin filaments in mouse fibroblasts [161], they have been used to detect a vast array of proteins in fixed tissue, by fluoroimmunoassays [186] as well as through flow cytometry [187]. QDs have enabled the detection of biological markers with high sensitivity. Streptavidin-coated QDs used in conjunction with biotinylated antibodies, either primary or secondary, have most commonly been used to label and detect proteins in cells and tissues [188]. Several research groups have investigated different conjugation systems for QD labeling of biological molecules. A comparison of sulfhydryl, amide, Fc-sugar, His-tag, and biotin-avidin binding showed

that, Fc-sugar and His-tag conjugation have greater site and staining specificity, higher fluorescence intensity, and lower background noise, with a better overall performance than other procedures [185]. However, streptavidin-biotin conjugation chemistry is the most practicable strategy, due to the availability of commercial streptavidin-QDs/biotinylated antibodies and the existence of pre-established protocols for their use requiring only minor optimization.

An important advantage of using QDs is the suitability for multiplex detection due to their tuneable narrow symmetrical emission and wide excitation [189]. However, there are two problems frequently encountered in multiplex studies: antibody cross-reactivity and poor signal separation. The former can be addressed by using either different antibody species or different methods for detecting different antigens, while the latter requires high-quality image analysis. Multiplexing of QDs has been used to simultaneously detect several biomarkers by sequential staining for each antibody (see Fig. 1.7) [190]. The tissue is first treated with the primary antibody-recognizing marker protein. The marker protein-bound primary antibody is then labeled with streptavidin-coated QDs through the biotinylated secondary antibody. Avidin-biotin blocks are applied after labeling each marker with QDs and before treatment with primary antibody for the next protein marker [190]. However, the procedure is time-consuming and there is a possibility of transfer of streptavidin-coated QDs between different secondary antibodies [191].

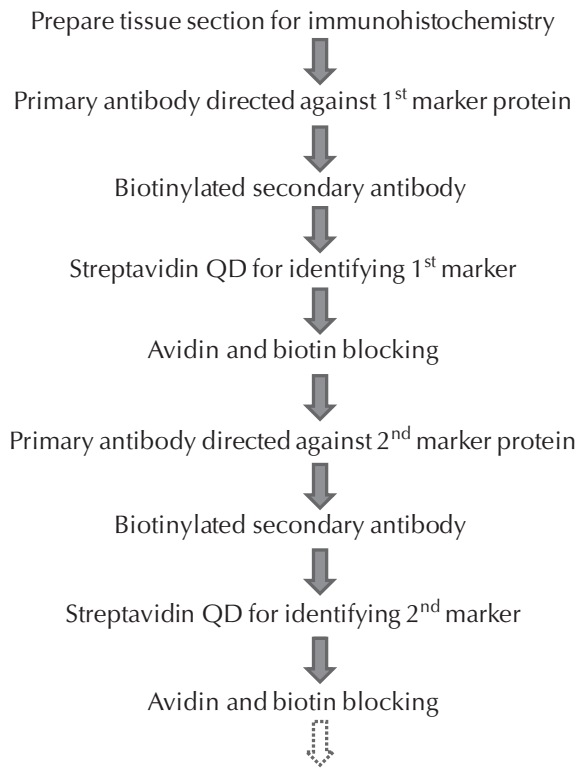

Fig. 1.7 Sequential staining for multiplex imaging using streptavidin QDs.

Multiplex QDs have been evaluated to study markers in needle core biopsies in clinics in order to provide personalized treatment [192]. This technique provides a quantitative measurement of several markers in small-sized tissue samples. A workflow for the use of multiplex QD imaging in clinical practice has been proposed in some studies [189]. This is essential if QDs are to become clinically more useful. A dedicated software package called Q-IHC, for the integration of traditional and QD-based IHC, enables quantitative image analysis of each of the biomarkers [185].

With the advent of high-throughput platforms for genomics, proteomics, and transcriptomics, there is an increasing need to measure an expanding number of biomarkers *in vivo* in biological samples that may include proteins, DNA, or mRNA. QD-labeled oligonucleotide probes have been employed to identify mutations by fluorescence *in situ* hybridization (FISH) [193]. Streptavidin-conjugated QDs have also been successfully used in FISH studies on the chromosomes of humans [194], mice [195], plants [196], and microorganisms such as *Escherichia coli* [197]. Streptavidin-QDs with biotinylated probes have been used to study mRNA expression levels in fresh animal tissue both for single marker studies [198] and for duplex/multiplex analyses [199]. However, almost all clinical pathology samples are stored as formalin-fixed paraffin-embedded (FFPE) samples. A recent study has demonstrated the use of QDs for FISH in FFPE samples and addressed the problems associated with use of these samples in place of fresh tissues [200]. Although the use of streptavidin-coated QDs for ISH is highly prevalent, there is concern due to stoichiometric

rearrangement. Amine-modified oligonucleotide probes can be covalently attached to the carboxyl terminals on polymer-coated QDs using EDC, allowing direct stable conjugation of a probe with QD [201].

However, multiplex imaging using either antibody or DNA probes results in the generation of multicolored images. In order to detect multiple markers simultaneously, it is necessary to carry out color resolution to identify and quantify individual signals. Hyperspectral imaging involves the collection of a complete spectrum at every location in an image plane, from which an entire spectral profile can be generated for each pixel in the image field [202]. The spectral information obtained from each pixel can then be used to discriminate between noise and signal, as well as between fluorescent signals from different markers [203].

High fluorescence intensity and photostability of QDs have enabled their use in single molecule imaging. Labeling of cellular proteins such as epidermal growth factor (EGF) [204], CD44 [205], protease-activated receptor-1 (PAR-1) [206], etc. with QDs enabled the tracking of these proteins in live cells, providing valuable mechanistic insights. For example, the ability to visualize movement of PAR-1 on the tumor cells during different stages of metastasis showed that membrane fluidity of tumor cells increases during intravasation, reaches a peak in vessels, being particularly high at pseudopodia-like membrane projections, and then decreases during extravasation [206]. This technique will thus help in the visualization of complex interactions between biomolecules and the observation of cellular processes at the molecular level.

QDs have been used extensively in live animal imaging, particularly using illumination with near-infrared and infrared light, which enables penetration of skin and tissue. The high brightness of QDs permits their detection in deep sites. Live mammalian cells labeled with large amounts of QDs have been used to study embryogenesis [207], cancer metastasis [208], stem cells [209], and lymphocyte homing [210]. The use of QDs for lymph node mapping has been demonstrated in lower mammals [211], raising the possibility of intraoperative use in humans [212], particularly in breast cancer. QDs have also been used to image blood vessels in live mice and to track cancer metastasis [208]. Live animal imaging enables real-time longitudinal studies without frequent animal sacrifice. QDs conjugated to luciferase are endowed with the ability to self-illuminate, which allows deep tissue visualization that otherwise would have low incident light [213]. This approach also eliminates tissue autofluorescence and thus improves sensitivity.

1.4.3 Integrated QDs

Unlike the QDs used as labels in imaging, an integrated QD is one that is present in a system throughout the analysis, and simultaneously serves as a platform for biodetection as well as a transducer of a recognition event by fluorescence resonance energy transfer (FRET) [214], bioluminescence resonance energy transfer (BRET) [215], charge transfer quenching [216], and electrochemiluminescence (ECL) [217]. Integrated QDs have found several applications in sensing biomolecules, including the detection of small molecules using enzyme-linked methods [218] or aptamer affinity probes [219], detection of proteins via immunoassays [217] or aptamers [216], nucleic acid hybridization assays [214], and protease or nuclease activity assays [215].

1.4.4 Photodynamic therapy

Photodynamic therapy (PDT) is a less invasive cancer treatment strategy that involves the irradiation of tumor tissue with low-energy electromagnetic waves, typically visible or near-infrared (NIR) light, after treatment with a photosensitizer (PS). The PS absorbs the incident photon, gets excited and then transfers the energy to molecular oxygen present ubiquitously in the body, leading to the formation of singlet oxygen. Singlet oxygen is a very reactive chemical species that will induce apoptosis or necrosis of tumor cells in the vicinity by damaging key cell organelles such as mitochondria. The high photostability, broad absorption spectrum, and large two-photon absorption cross-section of QDs are great advantages for photoactivation using visible and NIR light sources [80]. QDs also produce reactive oxygen intermediates (ROI) [220] and reactive nitrogen species (RNS)

[221] upon photoactivation, and thus cause lysosomal damage [221] and DNA breakage [220, 221]. QDs have thus been evaluated for potential applications in PDT. However, the efficiency of ROI production by QDs is far inferior to that of conventional PS drugs. Since the pros and cons of QDs and PS drugs are complementary to each other, several conjugates/hybrids of QDs and conventional PS drugs have been investigated as new-generation drugs for PDT [80].

1.4.5 Drug delivery

QDs have also been investigated extensively for drug delivery. There is a growing interest in recent times for producing multimodal QDs capable of both *in vivo* tumor imaging and drug delivery [79, 222]. QDs conjugated to both a tumor-targeting ligand (an antibody) and the drug molecule can effectively serve this purpose. For example, QDs conjugated to anti-HER2 antibody and doxorubicin-loaded liposomes exhibited significant anticancer activity in HER2-overexpressing breast cancer cells, and enabled tumor cell imaging [79].

1.5 Toxicity

Nanotechnology is an emerging field that is likely to change the way almost everything – from drugs to computers to clothing to objects not yet imagined – is designed and manufactured. Nanomaterials have the potential to transform our everyday lives through the development of new technologies including advanced medical imaging and novel treatment strategies. However, a flurry of disturbing reports concerning the toxicity of NPs have recently surfaced [223–274]. With the widespread use of NPs, there is also a danger of unintended exposure, apart from that due to their intentional use in diagnostics and therapeutics. On the other hand, the resources and efforts directed towards understanding the toxicity of NPs is not keeping pace with the development of new nanomaterials. The knowledge gaps related to health risks may create liabilities that could stunt the development and exploitation of beneficial NPs. Several factors influence the toxicity of NPs to the human body: the properties of nanomaterials themselves, contaminants and coatings of NPs, and host factors (see Table 1.1). We discuss here in some detail the toxicity of the most extensively used metallic and carbon-based nanomaterials, and quantum dots.

Table 1.1 Factors influencing toxicity of nanomaterials.

PROPERTIES OF NANOPARTICLES
Size Generally, the smaller the size, the greater the toxicity
Shape For example, fullerenes are more toxic than CNTs
Surface Defects and redox status of NPs adversely influence toxicity
Agglomeration NPs with a tendency to clump in physiological conditions are more toxic
CONTAMINANTS AND COATINGS
Contaminants For example, metal impurities incorporated during CNT synthesis increase toxicity
Capping ligands Generally, more hydrophilic ligands increase the toxicity of NPs
PEGylation Reduces toxicity
Peptide coating Reduces toxicity
HOST FACTORS
Route of exposure Inhalation induces greater toxicity than ingestion and skin contact
Sequestration Accumulation of NPs in tissues enhances toxicity
Intracellular uptake Intracellular uptake of NPs tends to induce cytotoxicity
Rate of elimination A slower rate of elimination leads to increased toxicity

1.5.1 Toxicity of metallic NPs

1.5.1.1 AgNPs

Nanosilver has been proposed for extensive use in biomedical applications such as therapeutics [23, 25, 26, 30, 37, 38], as antimicrobial agents [24, 29, 31, 103–105], and as fluorescent labels [105, 108]. Despite rapid progress and early acceptance of nano-biotechnology as a translational research concept, the possible risk of adverse health effects following prolonged exposure to NPs at various concentration levels in humans, and the accompanying toxicological and environmental issues need to be raised. There has been continuous debate on the advantages and disadvantages of the use of silver products in health care and medicine [37]. Probably one of the most widely reported side-effects of silver products is argyria. Argyria occurs when subdermal silver is deposited in skin microvessels, resulting in an irreversible gray to black coloration of the skin [223]. This permanent discoloration is not physically harmful but remains an inherently serious cosmetic problem [37]. There are also some reports of kidney toxicity and cytotoxicity [224]. Liver toxicity has also been observed following acute silver toxicity due to nanocrystalline silver [225]. *In vivo* experiments in rats have clearly established lung function changes and inflammation [226]. AgNPs stabilized with starch and BSA induce distinct developmental defects in zebrafish embryos [227]. Recent reports have established the involvement of the mitochondria-dependent Jun N-terminal kinase (JNK) pathway in AgNP toxicity [228]. Recently a research group has unraveled the cytotoxicity and genotoxicity of AgNPs [229]. They made an effort to understand the various steps in AgNP toxicity by studying the effect of starch-coated AgNPs on cell viability, ATP production, DNA damage, chromosomal aberrations, and cell cycle. The DNA damage, chromosomal aberrations, and cell cycle arrest raised concerns about safety associated with applications of the AgNPs. Therefore, understanding the kinetics and toxicity of silver NPs *in vivo* is very important in the context of the underlying medical debate regarding the safety of nanosilver and nanomaterials coated with silver.

Recently, Stensberg and co-workers have provided an extensive discussion on current research on the transport, activity, and fate of AgNPs at the cellular and organism level [230]. The authors proposed several mechanisms of cytotoxcity based on such studies, as well as new opportunities for investigating the uptake and fate of AgNPs, establishing better models to assess long-term effects *in vivo*. But there are also reports to suggest that silver in lower concentrations is non-toxic to human cells. The epidemiological history of silver has established non-toxicity in normal use [37]. Thus, it is our opinion that these are questions that need to be urgently answered before people rush to join the nanosilver boom.

1.5.1.2 Gold nanoparticles

Although AuNPs are composed of an inert material and have extraordinary properties that make them useful for a wide array of biomedical applications [17, 19, 21, 22, 27, 35, 36, 112, 116, 121–124], biocompatibility issues need to be addressed. Several groups have examined the cellular uptake and toxicity of AuNPs. Cells exposed to AuNPs will incorporate the particles (similar to nanoparticles of other materials) and store them inside the cells in perinuclear compartments: vesicular structures close to the cell nucleus [231, 232]. Due to particle internalization, cells or tissues in contact with AuNPs will be exposed to the particles for extended periods of time. Inflammatory effects in tissues caused by AuNPs have been demonstrated. These results indicate that kinetics and saturation concentrations are highly dependent on the physical dimensions of the nanoparticle. Wang *et al*. have investigated shape- and size-dependent cellular uptake and cytotoxicity of Au nanomaterials on human skin HaCaT keratinocytes [233, 234]. However, in cell culture experiments, AuNPs are regarded as biocompatible and acute cytotoxicity has not been observed so far. Connor *et al*. [235] have examined the uptake and potential toxicity of a series of gold AuNPs in human leukemia cells. Results suggest that spherical AuNPs with a variety of surface modifiers are not inherently toxic to human cells, despite being taken up into cells [235].

On the other hand, there are a few examples of toxic effects related to the nature of Au, which might depend on the cell line or cell type [232, 236]. For example, 33 nm citrate-capped gold nanospheres were found to be non-toxic to baby hamster

kidney and human hepatocellular liver carcinoma cells, but were cytotoxic to a human carcinoma lung cell line, as reported by Patra *et al*. (2007) [232]. Gold cytotoxicity also depends on surface chemistry [237], and on the particle size [238]. Goodman *et al*. investigated the toxicity of AuNPs functionalized with both cationic and anionic surface groups in three different cell types. The results suggest that cationic particles are generally toxic at much lower concentrations than anionic particles, which they relate to the electrostatic interaction between the cationic nanoparticles and the negatively charged cell membranes. The toxicity of the AuNPs is related to their interactions with the cell membrane, a feature initially mediated by their strong electrostatic attraction to the negatively charged bilayer.

1.5.2 Toxicity of carbon nanomaterials

The demand for CNs is increasing rapidly in electrical, mechanical, health, and medical applications due to their thermal, electrical, optical, and other properties. The sustained massive investment worldwide in CN production and application needs to be accompanied by a thorough understanding of the occupational health, public safety, and environmental implications of these nanomaterials. Concern over possible harmful effects of nanomaterials has stimulated the advent of nanotoxicology as a significant research discipline. The literature is full of reports that carbon nanomaterials can cause *in vitro* and *in vivo* toxicity [239]. Most of the *in vivo* toxicity data have been generated from studies using CNTs. Animal studies have shown that exposure to nanotubes can cause inflammation, fibrosis, epithelioid granuloma formation in lungs [240–242], cellular cytotoxicity, and cardiopulmonary and vascular irregularities [243–245]. CNTs are also known to induce oxidative stress in human keratinocytes via nuclear factor kappa-B (NF-κB) [245]. A recent report by Porter and colleagues discusses the challenges associated with characterizing the toxicity of CNT and the need for complementary nanometrology to relate their physiochemical properties with their toxicity [246]. The authors suggest a combination of high-resolution electron microscopy techniques and cell viability assays to understand the cytotoxic mechanisms of the targeting site and stability of carbon nanotubes inside cells and tissues.

In other recent reports, carbon nanomaterials were found to adversely affect the platelets, an important component of circulatory system responsible for blood clotting and hemostasis [244, 247, 248]. Nanocarbon material such as SWNTs (single-walled nanotubes), MWNTs (multi-walled nanotubes), and mixed carbon nanoparticles (MCN) were found to have the ability to aggravate platelet aggregation [244], which may lead to deadly consequences such as stroke, myocardial infarction, and deep vein thrombosis [249–251]. Enhanced aggregation of platelets by different nanocarbons has been suggested to be the outcome of extracellular calcium influx into the cell [248].

However, to date, relatively few studies are available in the literature concerning the toxicity of graphene to cells or living organisms [252–256]. *In vitro* studies have demonstrated that, GO induces a marginal decrease in cell viability at higher doses and can elicit concentration-dependent cytotoxicity in A549 cells and PC12 cells [252, 253] mediated through oxidative stress and apoptosis. The shape of graphene sheets or their agglomeration may be important factors contributing to graphene toxicity. Animal studies have indicated that GO could induce severe cytotoxicity in a dose- and time-dependent manner, and can enter into the cytoplasm and nucleus, decreasing cell adhesion, inducing cell floating and apoptosis [254]. GO can enter into lung tissue, inducing inflammation and subsequent granuloma formation. Further comparative studies suggest that cells respond differently to reduced GO and carbon nanotubes, which may be attributed to their distinct nanotopographic features [255]. The reduced GO film is biocompatible with all tested cells, implying its potential application in biology. Recently we have demonstrated that GO can potentially induce integrin-mediated platelet aggregation both *in vitro* and *in vivo* [257]. Src and Syk tyrosine kinases were found to play key roles in GO-induced platelet activation. From comparative studies with reduced GO, we inferred that the charge distribution on the surface of GO regulates its capability to interact with cells and activate and aggregate platelets.

Surface characteristics of nanomaterials, such as shape, aggregate formation, coating, and functionalization, may be deciding factors for their adverse

toxic effects. Toxicity depends upon the surface area/mass ratio and retention time of the particles – particles having a larger surface area and higher retention time have greater contact with the cell membrane, and hence have a greater capacity for adsorption and transport into cells. Compared with CNTs, whose toxicity may be attributed to their water insolubility and tendency to form aggregates, the more water-dispersible graphene can serve as a less toxic material for applications in physiological systems. However, it would be advisable to critically assess the adverse prothrombotic and cytotoxic effects of GO before exploiting its biomedical potential as a therapeutic and diagnostic tool.

1.5.3 QD toxicity

The toxicity of heavy metals to mammalian cells is well documented [258–260]. Hence, the presence of a heavy metal core in QDs raises serious concerns about their potential toxicity. There has been an explosion of studies on potential applications of QDs in biological imaging both *in vitro* and *in vivo*, which has led to the accumulation of a wealth of information on the subject. On the other hand, the issue of their toxicity has received little attention. The lack of adequate knowledge on *in vivo* toxicity of QDs has precluded their use in humans despite having immense potential for applications in medical imaging.

QDs have successfully been used to track embryonic cells [261], T cells, dendritic cells [262], and mesenchymal stem cells [263] *in vivo* without any significant effect on the viability, morphology, function, or differentiation of these cells. QDs injected into the circulation of an animal model in order to target lung vasculature or tumor tissue did not induce any toxicity [264]. However, they have been found to activate human primary monocytes *in vitro* as well as inducing neutrophil infiltration in lungs *in vivo* upon repeated intravenous injections [265]. QDs have also been found to be toxic to porcine renal proximal tubule cells through the induction of autophagic cell death [266]. In addition, the dissolution of the heavy metal core by photolysis or oxidation has been demonstrated, with resultant heightened toxicity [267]. Although it is possible to shield the heavy metal core by ligand capping, some studies have reported toxicity due to these capping ligands, specifically MPA [268, 269]. An exciting solution to this issue is the use of non-toxic QD preparations, such as Si or SiC [270, 271]. Detoxifying agents such as glutathione [272] or gelatin [273], and peptide coating [274] have been found to reduce toxicity. Despite these preliminary reports, there is an urgent need to comprehensively investigate the toxicity of QDs both *in vitro* and *in vivo*, so that safer QD preparations may be developed.

References

1. Feynman RP. There's plenty of room at the bottom. *Eng. Sci. (CalTech)* **23**, 22–36 (1960).
2. Han M, Gao X, Su JZ , Nie S. Quantum-dot-tagged microbeads for multiplexed optical coding biomolecules. *Nat. Biotechnol.* **19**, 631–5 (2001).
3. Kamat PV. Photophysical, photochemical and photocatalytic aspects of metal nanoparticles. *J. Phys. Chem. B* **106**, 7729–44 (2002).
4. Katz E, Willner I. Integrated nanoparticle-biomolecule hybrid systems: Synthesis, properties, and applications. *Angew. Chem. Int. Ed.* **43**, 6042–108 (2004).
5. Pagona G, Tagmatarchis N. Carbon nanotubes: Materials for medicinal chemistry and biotechnological applications. *Curr. Med. Chem.* **13**, 1789–98 (2006).
6. Tang XW, Bansaruntip S, Nakayama N, Yenilmez E, Chang YL, Wang Q. Carbon nanotube DNA sensor and sensing mechanism. *Nano Lett.* **6**, 1632–6 (2006).
7. Sun X, Liu Z, Welsher K, Robinson JT, Goodwin A, Zaric S, Dai H. Nano-graphene oxide for cellular imaging and drug delivery. *Nano Res.* **1**, 203–12 (2008).
8. Robinson JT, Tabakman SM, Liang Y, Wang H, Sanchez Casalongue H, Vinh D, Dai H. Ultrasmall reduced graphene oxide with high near-infrared absorbance for photothermal therapy. *J. Am. Chem. Soc.* **133**, 6825–31 (2011).
9. Gaffet E, Tachikart M, El Kedim O, Rahouadj R. Nanostructural materials formation by mechanical alloying: Morphologic analysis based on transmission and scanning electron microscopic observations. *Mater. Charact.* **36**, 185–90 (1996).
10. Amulyavichus A, Daugvila A, Davidonis R, Sipavichus C. Study of chemical composition of nanostructural materials prepared by laser cutting of metals., *Fizika Metallov I Metallovedenie* **85**, 111–17 (1998).

11. Bonnemann H, Braun G, Brijoux W. Nanoscale colloidal metals and alloys stabilized by solvents and surfactants: Preparation and use as catalyst precursors. *J. Organometallic Chem.* **520**, 143–62 (1996).
12. Zameer S, Yutaka I, Masahiro S, Hajime K, Yukiya H, Toshirou Y, Takako N, Hironobu KA, Kenji A. Morphology and size-controlled synthesis of silver nanoparticles in aqueous surfactant polymer solutions. *Colloid Polym. Sci.* **286**, 403–10 (2008).
13. Ghosh KK, Kolay S. Preparation of Ag nanoparticles in surfactant solution. *J. Dispersion Sci. Technol.* **29**, 676–81 (2008).
14. Brettreich M, Hirsch A. A highly water-soluble dendro[60]fullerene. *Tetrahedron Lett.* **39**, 2731–4 (1998).
15. Zeng L, Alemany LB, Edwards CL, Barron AR. Demonstration of covalent sidewall functionalization of single wall carbon nanotubes by NMR spectroscopy: Side chain length dependence on the observation of the sidewall sp3 carbons. *Nano Res.* **1**, 72–88 (2008).
16. Mohanty N, Berry V. Graphene-based single-bacterium resolution biodevice and DNA transistor: Interfacing graphene derivatives with nanoscale and microscale biocomponents. *Nano Lett.* **8**, 4469–76 (2008).
17. Murphy CJ, Gole AM, Stone JW, Sisco PN, Alkiany AM, Goldsmith EC, Baxter SC. Gold nanoparticles in biology: Beyond toxicity to cellular imaging. *Acc. Chem. Res.* **41**, 1721–30 (2008).
18. Cao YWC, Jin RC, Mirkin CA. Nanoparticles with Raman spectroscopic fingerprints for DNA and RNA detection. *Science* **297**, 1536–40 (2002).
19. Daniel MC, Astruc D. Gold nanoparticles: Assembly, supramolecular chemistry, quantum-sized-related properties, and applications towards biology, catalysis and nanotechnology. *Chem. Rev.* **104**, 293–346 (2004).
20. Fritzsche W, Taton TA. Metal nanoparticles as labels for heterogeneous, chip-based DNA detection. *Nanotechnology* **14**, R63–R73 (2003).
21. Ghosh P, Han G, De M, Kim CK, Rotello VM. Gold nanoparticles in delivery applications. *Adv. Drug Delivery Rev.* **60**, 1307–15 (2008).
22. Rosi NL, Giljohann DA, Thaxton CS, Lytton-Jean AKR, Han MS, Mirkin CA. Oligonucleotide modified gold nanoparticles for intracellular gene regulation. *Science* **312**, 1027–30 (2006).
23. Shrivastava S, Bera T, Singh SK, Singh G, Ramachandrarao P, Dash D. Characterization of antiplatelet properties of silver nanoparticles. *ACS Nano* **3**, 1357–64 (2009).
24. Shrivastava S, Bera T, Roy A, Singh G, Ramachandrarao P, Dash D. Characterization of enhanced antibacterial effects of novel silver nanoparticles. *Nanotechnology* **18**, 225103–11 (2007).
25. Darouiche RO. Anti-infective efficacy of silver-coated medical prostheses. *Clin. Infect Dis.* **29**, 1371–7 (1999).
26. Elechiguerra JL, Burt JL, Morones JR, Camacho-Bragado A, Gao X, Lara HH, Yacaman MJ. Interaction of silver nanoparticles with HIV-1. *J. Nanobiotechnol.* **3**, 6 (2005).
27. Huff TB, Tong L, Zhao Y, Hansen MN, Cheng JX, Wei A. Hyperthermic effects of gold nanorods on tumor cells. *Nanomedicine* **2**, 125–32 (2007).
28. Jain P, Pradeep T. Potential of silver nanoparticle-coated polyurethane foam as an antibacterial water filter. *Biotechnol. Bioeng.* **90**, 59–63 (2005).
29. Kim JS, Kuk E, Yu KN, Kim JH, Park SJ, Lee HJ. Antimicrobial effects of silver nanoparticles. *Nanomedicine: NBM* **3**, 95–101 (2007).
30. Klasen HJ. A historical review of the use of silver in the treatment of burns. II. Renewed interest for silver. *Burns* **26**, 131–8 (2000).
31. Li P, Li J, Wu C, Wu Q, Li J. Synergistic antibacterial effects of β-lactam antibiotic combined with silver nanoparticles. *Nanotechnology* **16**, 1912–17 (2005).
32. Li Y, Leung P, Yao L, Song QW, Newton E. Antimicrobial effect of surgical masks coated with nanoparticles. *J. Hosp. Infec.* **62**, 58–63 (2006).
33. Lowery AR, Gobin AM, Day ES, Halas NJ, West JL. Immunonanoshells for targeted photothermal ablation of tumor cells. *Int. J. Nanomed.* **1**, 149–54 (2006).
34. O'Neal DP, Hirsch LR, Halas NJ, Payne JD, West JL. Photo-thermal tumor ablation in mice using near infrared-absorbing nanoparticles. *Cancer Lett.* **209**, 171 (2004).
35. Pissuwan D, Valenzuela SM, Cortie MB. Therapeutic possibilities of plasmonically heated gold nanoparticles. *Trends Biotechnol.* **24**, 62–7 (2006).
36. Rojo J, Diaz V, de la Fuente JM, Segura I, Barrientos AG, Riese HH, Bernad A, Penades S. Gold glyconanoparticles as new tools in antiadhesive therapy. *ChemBioChem* **5**, 291–7 (2004).
37. Silver S, Phung LT, Silver G. Silver as biocides in burn and wound dressings and bacterial resistance to silver compounds. *J. Ind. Microbiol. Biotechnol.* **33**, 627–34 (2006).
38. Stevens KNJ, Crespo-Biel O, van den Bosch EEM, Dias AA, Knetsch MLW, Aldenhoff YBJ, van der Veen FH, Maessen JG, Stobberingh EE, Koole LH. The relationship between the antimicrobial effect of catheter coatings containing silver nanoparticles and the coagulation of contacting blood. *Biomaterials* **30**, 3682–90 (2009).
39. Schinazi RF, Sijbesma R, Srdanov G, Hill CL, Wudl F. Synthesis and virucidal activity of a water-soluble,

configurationally stable, derivatized C60 fullerene. *Antimicrob. Agents Chemother.* **37**, 1707–10 (1993).
40. Tsao N, Kanakamma PP, Luh TY, Chou CK, Lei HY. Inhibition of *Escherichia coli*-induced meningitis by carboxyfullerene. *Antimicrob. Agents Chemother.* **43**, 2273–7 (1999).
41. Tsao N, Luh TY, Chou CK, Wu JJ, Lin YS, Lei HY. Inhibition of group A *Streptococcus* infection by carboxyfullerene. *Antimicrob. Agents Chemother.* **45**, 1788–93 (1999).
42. Bosi S, Da Ros T, Castellano S, Banti E, Prato M. Antimycobacterial activity of ionic fullerene derivatives. *Bioorg. Med. Chem. Lett.* **10**, 1043–5 (2000).
43. Tabata Y, Murakami Y, Ikada Y. Photodynamic effect of polyethylene glycol-modified fullerene on tumor. *Jpn. J. Cancer Res.* **88**, 1108–16 (1997).
44. Tabata Y, Murakami Y, Ikada Y. Antitumor effect of poly (ethylene glycol)-modified fullerene. *Fullerene Sci. Technol.* **5**, 989–1007 (1997).
45. Miyata N, Yamakoshi T. In: Kadish KM, Ruoff RS, editors. *Fullerenes: Recent Advances in the Chemistry and Physics of Fullerenes and Related Materials*. Pennington, NJ: Electrochemical Society, 345–57 (1997).
46. Dugan LL, Lovett E, Cuddihy S, Ma B, Lin T, Choi DW. Carboxyfullerenes as neuroprotective antioxidants. In: Kadish KM, Ruoff RS, editors. *Fullerenes: Chemistry, Physics, and Technology*. New York: John Wiley & Sons, 467–80 (2000).
47. Cai X, Jia H, Liu Z, Hou B, Luo C, Feng Z, Li W, Liu J. Polyhydroxylated fullerene derivative C(60)(OH)(24) prevents mitochondrial dysfunction and oxidative damage in an MPP(+)-induced cellular model of Parkinson's disease. *J. Neurosci. Res.*, **86**, 3622–34 (2008).
48. Kam NWS, Liu Z, Dai H. Functionalization of carbon nanotubes via cleavable disulfide bonds for efficient intracellular delivery of siRNA and potent gene silencing. *J. Am. Chem. Soc.* **127**, 12492–3 (2005).
49. Liu Z, Chen K, Davis C, Sherlock S, Cao Q, Chen X, Dai H. Drug delivery with carbon nanotubes for *in vivo* cancer treatment. *Cancer Res.* **68**, 6652–60 (2008).
50. Pantarotto D, Briand JP, Prato M, Bianco A. Translocation of bioactive peptides across cell membranes by carbon nanotubes. *Chem. Commun.* **2004**, 16–17 (2004).
51. Liu Z, Sun X, Nakayama N, Dai H. Supramolecular chemistry on water-soluble carbon nanotubes for drug loading and delivery. *ACS Nano* **1**, 50–6 (2007).
52. Zavaleta C, De La Zerda A, Liu Z, Keren S, Cheng Z, Schipper M, Chen X, Dai H, Gambhir SS. Noninvasive Raman spectroscopy in living mice for evaluation of tumor targeting with carbon nanotubes. *Nano Lett.* **8**, 2800–5 (2008).
53. Chakravarty P, Marches R, Zimmerman NS, Swafford AD, Bajaj P, Musselman IH, Pantano P, Draper RK, Vitetta ES. Thermal ablation of tumor cells with antibody-functionalized single-walled carbon nanotubes. *Proc. Natl. Acad. Sci. USA* **105**, 8697–702 (2008).
54. Kam NWS, O'Connell M, Wisdom JA, Dai H. Carbon nanotubes as multifunctional biological transporters and near-infrared agents for selective cancer cell destruction. *Proc. Natl. Acad. Sci. USA* **102**, 11600–5 (2005).
55. Liu Z, Tabakman S, Welsher K, Dai H. Carbon nanotubes in biology and medicine: *In vitro* and *in vivo* detection, imaging and drug delivery. *Nano Res.* **2**, 85–120 (2009).
56. Fu CC, Lee HY, Chen K, Lim TS, Wu HY, Lin PK, Wei PK, Tsao PH, Chang HC, Fann W. Characterization and application of single fluorescent nanodiamonds as cellular biomarkers. *Proc. Natl. Acad. Sci. USA* **104**, 727–32 (2007).
57. Chang YR, Lee HY, Chen K, Chang CC, Tsai DS, Fu CC, Lim TS, Tzeng YK, Fang CY, Han CC, et al. Mass production and dynamic imaging of fluorescent nanodiamonds. *Nat. Nanotechnol.* **3**, 284–8 (2008).
58. Yu SJ, Kang MW, Chang HC, Chen KM, Yu YC. Bright fluorescent nanodiamonds: No photobleaching and low cytotoxicity. *J. Am. Chem. Soc.* **127**, 17604–5 (2005).
59. Kong XL, Huang LC, Hsu CM, Chen WH, Han CC, Chang HC. High-affinity capture of proteins by diamond nanoparticles for mass spectrometric analysis. *Anal. Chem.* **77**, 259–65 (2005).
60. Kossovsky N, Gelman A, Hnatyszyn HJ, Rajguru S, Garrell RL, Torbati S, Freitas SS, Chow GM. Surface-modified diamond nanoparticles as antigen delivery vehicles. *Bioconjug. Chem.* **6**, 507–11 (1995).
61. Huang H, Pierstorff E, Osawa E, Ho D. Active nanodiamond hydrogels for chemotherapeutic delivery. *Nano Lett.* **7**, 3305–14 (2007).
62. Huang LC, Chang HC. Adsorption and immobilization of cytochrome c on nanodiamonds. *Langmuir* **20**, 5879–84 (2004).
63. Liu Y, Yu D, Zeng C, Miao Z, Dai L. Biocompatible graphene oxide-based glucose biosensors. *Langmuir* **26**, 6158–60 (2010).
64. Wang Y, Li YM, Tang LH, Lu J, Li JH. Application of graphene-modified electrode for selective detection of dopamine. *Electrochem. Commun.* **11**, 889–92 (2009).
65. Sun X, Liu Z, Welsher K, Robinson JT, Goodwin A, Zaric S, Dai H. Nano-graphene oxide for cellular imaging and drug delivery. *Nano Res.* **1**, 203–12 (2008).
66. Peng C, Hu W, Zhou Y, Fan C, Huang Q. Intracellular imaging with a graphene-based fluorescent probe. *Small* **6**, 1686–92 (2010).

67. Liu Z, Robinson JT, Sun X, Dai H. PEGylated nanographene oxide for delivery of water insoluble cancer drugs. *J. Am. Chem. Soc.* **130**, 10876–7 (2008).
68. Hu W, Peng C, Luo W, Lv M, Li X, Li D, Huang Q, Fan C. Graphene-based antibacterial paper. *ACS Nano* **4**, 4317–23 (2010).
69. Akhavan O, Ghaderi E. Toxicity of graphene and graphene oxide nanowalls against bacteria. *ACS Nano* **4**, 5731–6 (2010).
70. Yang K, Zhang S, Zhang G, Sun X, Lee ST, Liu Z. Graphene in mice: Ultrahigh *in vivo* tumor uptake and efficient photothermal therapy. *Nano Lett.* **10**, 3318–23 (2010).
71. Robinson JT, Tabakman SM, Liang Y, Wang H, Casalongue HS, Vinh D, Dai H. Ultrasmall reduced graphene oxide with high near-infrared absorbance for photothermal therapy. *J. Am. Chem. Soc.* **133**, 6825–31 (2011).
72. Shan C, Yang H, Han D, Zhang Q, Ivaska A, Niu L. Water-soluble graphene covalently functionalized by biocompatible poly-L-lysine. *Langmuir* **25**, 12030–3 (2009).
73. Zrazhevskiy P, Gao X. Multifunctional quantum dots for personalized medicine. *Nano Today* **4**, 414–28 (2009).
74. Xing Y, Xia Z, Rao J. Semiconductor quantum dots for biosensing and in vivo imaging. *IEEE Tran. Nanobioscience* **8**, 4–12 (2009).
75. Lidke DS, Nagy P, Heintzmann R, Arndt-Jovin DJ, Post JN, Grecco HE, Jares-Erijman EA, Jovin TM. Quantum dot ligands provide new insights into erbB/HER receptor-mediated signal transduction. *Nat. Biotechnol.* **22**, 198–203 (2004).
76. Bentolila LA, Weiss S. Single-step multicolor fluorescence in situ hybridization using semiconductor quantum dot-DNA conjugates. *Cell Biochem. Biophys.* **45**, 59–70 (2006).
77. Medintz IL, Mattoussi H. Quantum dot-based resonance energy transfer and its growing application in biology. *Phys. Chem. Chem. Phys.* **1**, 17–45 (2009).
78. Medintz IL, Pons T, Trammell SA, Grimes AF, English DS, Blanco-Canosa JB, Dawson PE, Mattoussi H. Interactions between redox complexes and *semiconductor quantum dots* coupled via a peptide bridge. *J. Am. Chem. Soc.* **130**, 16745–56 (2008).
79. Weng KC, Noble CO, Papahadjopoulos-Sternberg B, Chen FF, Drummond DC, Kirpotin DB, Wang D, Hom YK, Hann B, Park JW. Targeted tumor cell internalization and imaging of multifunctional quantum dot-conjugated immunoliposomes in vitro and in vivo. *Nano Lett.* **8**, 2851–7 (2008).
80. Samia ACS, Chen XB, Burda C. Semiconductor quantum dots for photodynamic therapy. *J. Am. Chem. Soc.* **125**, 15736–7 (2003).
81. Qiang Y, Antony J, Sharma A, Nutting J, Sikes D, Meyer D. Iron/iron oxide core-shell nanoclusters for biomedical applications. *J. Nanopart. Res.* **8**, 489–96 (2006).
82. Majewski P, Thierry B. Functionalized magnetite nanoparticles: Synthesis, properties, and bioapplications. *Crit. Rev. Solid State Mat. Sci.* **32**, 203–15 (2007).
83. Uhrich KE, Cannizzaro SM, Langer RS, Shakesheff KM. Polymeric systems for controlled drug release. *Chem. Rev.* **99**, 3181–98 (1999).
84. Makadia HK, Siegel SJ. Poly lactic-co-glycolic acid (plga) as biodegradable controlled drug delivery carrier. *Polymers* **3**, 1377–97 (2011).
85. Sailaja AK, Amareshwar P, Chakravarty P. Chitosan nanoparticles as a drug delivery system. *RJPBCS* **1**, 474–84 (2010).
86. Brandl M. Liposomes as drug carriers: A technological approach. *Biotechnol. Annu. Rev.* **7**, 59–85 (2001).
87. Samad A, Sultana Y, Aqil M. Liposomal drug delivery systems: An update review. *Curr. Drug Deliv.* **4**, 297–305 (2007).
88. Abraham SA, Waterhouse DN, Mayer LD, Cullis PR, Madden TD, Bally MB. The liposomal formulation of doxorubicin. *Methods Enzymol.* **391**, 71–97 (2005).
89. Almeida AJ, Souto E. Solid lipid nanoparticles as a drug delivery system for peptides and proteins. *Adv. Drug Deliv. Rev.* **59**, 478–90 (2007).
90. Tan Y, Dai Y, Li Y, Zhua D. Preparation of gold, platinum, palladium and silver nanoparticles by the reduction of their salts with a weak reductant – potassium bitartrate. *J. Mater. Chem.* **13**, 1069–75 (2003).
91. Mallick K, Witcomb MJ, Scurell MS. Polymer stabilized silver nanoparticles: A photochemical synthesis route. *J. Mater. Sci.* **39**, 4459–63 (2003).
92. Li Y, Duan X, Qian Y, Li Y, Liao H. Nanocrystalline silver particles: Synthesis, agglomeration, and sputtering induced by electron beam. *J. Colloid Interface Sci.* **209**, 347–9 (1999).
93. Bolander ME, Mukhopadhyay D, Sarkar G, Mukherjee P. The use of microorganisms for the formation of metal nanoparticles and their application. *Appl. Microbiol. Biotechnol.* **69**, 485–92 (2006).
94. Ahmad A, Mukherjee P, Mandal D, Senapati S, Islam Khan M, Kumar R, Sastry M. Enzyme mediated extracellular synthesis of CdS nanoparticles by the fungus *Fusarium oxysporum*. *J. Am. Chem. Soc.* **124**, 12108–9 (2002).
95. Mukherjee P, Senapati S, Mandal D, Ahmad A, Khan MI, Kumar R. Extracellular synthesis of gold nanoparticles by the fungus *Fusarium oxysporum*. *Chem. Biochem.* **3**, 461–3 (2002).

96. Ahmad A, Mukherjee P, Senapati S, Mandal D, Khan MI, Kumar R, Sastry M. Extracellular biosynthesis of silver nanoparticles using the fungus *Fusarium oxysporum*. *Colloids Surf. B* **28**, 313–18 (2003).
97. Kim YC, Park NC, Shin JS, Lee SR, Lee YJ, Moon DJ. Partial oxidation of ethylene to ethylene oxide over nanosized Ag/α-Al_2O_3 catalysts. *Catal. Today* **87**, 153–62 (2003).
98. Nicewarner-Pena SR, Freeman RG, Reiss BD, He L, Pena DJ, Walton ID, Cromer R, Keating CD, Natan MJ. Submicrometer metallic barcodes. *Science* **294**, 137–41 (2001).
99. O'Neal DP, Hirsch LR, Halas NJ, Payne JD, West JL. Photo-thermal tumor ablation in mice using near infrared-absorbing nanoparticles. *Cancer Lett.* **209**, 171 (2004).
100. Marimuthu S, Rahuman AA, Rajakumar G, Santhoshkumar T, Kirthi AV, Jayaseelan C, Bagavan A, Zahir AA, Elango G, Kamaraj C. Evaluation of green synthesized silver nanoparticles against parasites. *Parasitol. Res.* **108**, 1541–9 (2011).
101. Singh SK, Shrivastava S, Nayak M, Sinha ASK, Jagannadham MV, Dash D. Stabilization of protein by biocompatible nanoparticles of silver. *J. Bionanosci.* **3**, 88–96 (2009).
102. Klaus T, Joerger R, Olsson E, Granqvist CG. Silver-based crystalline nanoparticles, microbially fabricated. *Proc. Natl. Acad. Sci. USA* **96**, 13611–14 (1999).
103. Nanda A, Saravanan M. Biosynthesis of silver nanoparticles from *Staphylococcus aureus* and its antimicrobial activity against MRSA and MRSE. *Nanomed. Nanotechnol. Biol. Med.* **5**, 452–6 (2009).
104. Fayaz AM, Balaji K, Girilal M, Yadav R, Kalaichelvan PT, Venketesan R. Biogenic synthesis of silver nanoparticles and their synergistic effect with antibiotics: A study against Gram-positive and Gram-negative bacteria. *Nanomed. Nanotechnol. Biol. Med.* **6**, 103–9 (2010).
105. Morones JR, Elechiguerra JL, Camacho A, Holt K, Kouri JB, Ramirez JT, Yacaman MJ. The bactericidal effect of silver nanoparticles. *Nanotechnology* **16**, 2346–53 (2005).
106. Chen LQ, Xiao SJ, Peng L, Wu T, Ling J, et al. Aptamer-based silver nanoparticles used for intracellular protein imaging and single nanoparticle spectral analysis. *J. Phys. Chem. B* **114**, 3655–9 (2010).
107. Tian J, Wong KK, Ho CM, Lok CN, Yu WY, Che CM. Topical delivery of silver nanoparticles promotes wound healing. *Chem. Med. Chem.* **2**, 129–36 (2007).
108. Alivisatos AP. The use of nanocrystals in biological detection. *Nat. Biotechnol.* **22**, 47–51 (2004).
109. Ghadiali JE, Stevens MM. Enzyme-responsive nanoparticle systems. *Adv. Mater.* **20**, 4359–63 (2008).
110. Turkevich J, Stevenson PC, Hillier J. A study of the nucleation and growth processes in the synthesis of colloidal gold. *Disc. Faraday Soc.* **0**, 55–75 (1951).
111. Kimling J, Maier M, Okenve B, Kotaidis V, Ballot H, Plech A. Turkevich method for gold nanoparticle synthesis revisited. *J. Phys. Chem. B* **110**, 15700–7 (2006).
112. Giersig M, Mulvaney P. Preparation of ordered colloid monolayers by electrophoretic deposition. *Langmuir* **9**, 3408–13 (1993).
113. Brust M, Walker M, Bethell D, Schiffrin DJ, Whyman RJ. Synthesis of thiol-derivatized gold nanoparticles in a 2-phase liquid–liquid system. *J. Chem. Soc. Chem. Commun.* **7**, 801–2 (1994).
114. Sperling RA, Rivera Gil P, Zhang F, Zanella M, Parak WJ. Biological applications of gold nanoparticles. *Chem. Soc. Rev.* **37**, 1896–908 (2008).
115. Pellegrino T, Sperling RA, Alivisatos AP, Parak WJ. Gel electrophoresis of gold-DNA nanoconjugates. *J. Biomed. Biotechnol.* **2007**, 26796–804 (2007).
116. Liz-Marzán LM. Nanomaterials: Formation and color. *Mater. Today* **7**, 26–31 (2004).
117. El-Sayed MA. Some interesting properties of metals confined in time and nanometer space of different shapes. *Acc. Chem. Res.* **34**, 257–64 (2001).
118. Rosi NL, Mirkin CA. Nanostructures in biodiagnostics. *Chem. Rev.* **105**, 1547–62 (2005).
119. Huang X, El-Sayed IH, Qian W, El-Sayed MA. Cancer cell imaging and photothermal therapy in the near-infrared region by using gold nanorods. *J. Am. Chem. Soc.* **128**, 2115–20 (2006).
120. Stern MJ, Stanfield J, Kabbani W, Hsieh JT, Cadeddu JA. Selective prostate cancer thermal ablation with laser activated gold nanoshells. *J. Urol.* **179**, 748–53 (2008).
121. Thanh NT, Rosenzweig Z. Development of an aggregation-based immunoassay for anti-protein A using gold nanoparticles. *Anal. Chem.* **74**, 1624–8 (2002).
122. Zhang CX, Zhang Y, Wang X, Tang ZM, Lu ZH. Hyper-Rayleigh scattering of protein-modified gold nanoparticles. *Anal. Biochem.* **320**, 136–40 (2008).
123. Kroto HW, Heath JR, O'Brien SC, Curl RF, Smalley RE. C60: Buckminsterfullerene. *Nature* **318**, 162–3 (1985).
124. Iijima S. Helical microtubules of graphitic carbon. *Nature* **354**, 56–8 (1991).
125. Novoselov KS, Geim AK, Morozov SV, Jiang D, Zhang Y, Dubonos SV, Grigorieva IV, Firsov AA. Electric field effect in atomically thin carbon films. *Science* **306**, 666–9 (2004).
126. Eklund PC, Pradhan BK, Kim UJ, et al. Large-scale production of single-walled carbon nanotubes using ultrafast pulses from a free electron laser. *Nano Lett.* **2**, 561–6 (2002).

127. Nikolaev P, Bronikowski MJ, Bradley RK, et al. Gas-phase catalytic growth of single walled carbon nanotubes from carbon monoxide. *Chem. Phys. Lett.* **313**, 91–7 (1999).
128. Park SJ, Ruoff RS. Chemical methods for the production of graphenes. *Nat. Nanotechnol.* **4**, 217–24 (2009).
129. Brodie BC. Sur le poids atomique du graphite. *Ann. Chim. Phys.* **59**, 466–72 (1860).
130. Staudenmaier L. Verfahren zur Darstellung der Graphitsäure. *Ber. Dtsch. Chem. Ges.* **31**, 1481–99 (1860).
131. Hummers WS Jr, Offeman RE. Preparation of graphitic oxide. *J. Am. Chem. Soc.* **80**, 1339 (1958).
132. Rosca ID, Watari F, Uo M, Akaska T. Oxidation of multiwalled carbon nanotubes by nitric acid. *Carbon* **43**, 3124–31 (2005).
133. Zeng L, Alemany LB, Edwards CL, Barron AR. Demonstration of covalent sidewall functionalization of single wall carbon nanotubes by NMR spectroscopy: Side chain length dependence on the observation of the sidewall sp3 carbons. *Nano Res.* **1**, 72–88 (2008).
134. Gooding JJ, Wibowo R, Liu JQ, Yang WR, Losic D, Orbons S, Mearns FJ, Shapter JG, Hibbert DB. Protein electrochemistry using aligned carbon nanotube arrays. *J. Am. Chem. Soc.* **125**, 9006–7 (2003).
135. Guiseppi-Elie A, Lei CH, Baughman RH. Direct electron transfer of glucose oxidase on carbon nanotubes. *Nanotechnology* **13**, 559–64 (2002).
136. Patolsky F, Weizmann Y, Willner I. Long-range electrical contacting of redox enzymes by SWCNT connectors. *Angew. Chem. Int. Edn.* **43**, 2113–7 (2004).
137. Willner I. Biomaterials for sensors, fuel cells, and circuitry. *Science* **298**, 2407–8 (2002).
138. Chen RJ, Bangsaruntip S, Drouvalakis KA, Kam NWS, Shim M, Li YM, Kim W, Utz PJ, Dai HJ. Noncovalent functionalization of carbon nanotubes for highly specific electronic biosensors. *Proc. Natl. Acad. Sci. USA* **100**, 4984–9 (2003).
139. Tang XW, Bansaruntip S, Nakayama N, Yenilmez E, Chang YL, Wang Q. Carbon nanotube DNA sensor and sensing mechanism. *Nano Lett.* **6**, 1632–6 (2006).
140. Shao Y, Wang J, Wu H, Liu J, Aksay IA, Lin Y. Graphene based electrochemical sensors and biosensors: A review. *Electroanalysis* **22**, 1027–36 (2010).
141. Tang LH, Wang Y, Li YM, Feng HB, Lu J, Li JH. Preparation, structure and electrochemical properties of graphene modified electrode. *Adv. Funct. Mater.* **19**, 2782 (2009).
142. Alwarappan S, Erdem A, Liu C, Li CZ. Probing the electrochemical properties of graphene nanosheets for biosensing applications. *J. Phys. Chem. C* **113**, 8853 (2009).
143. Wang Y, Li YM, Tang LH, Lu J, Li JH. Application of graphene-modified electrode for selective detection of dopamine. *Electrochem. Commun.* **11**, 889 (2009).
144. Zhou M, Zhai YM, Dong SJ. Electrochemical sensing and biosensing platform based on chemically reduced graphene oxide. *Anal. Chem.* **81**, 5603 (2009).
145. Liu F, Young CJ, Seo TS. Graphene oxide arrays for detecting specific DNA hybridization by fluorescence resonance energy transfer. *Biosensors Bioelectronics* **25**, 2361–5 (2010).
146. Chang H, Tang L, Wang Y, Jiang J, Li J. Graphene fluorescence resonance energy transfer aptasensor for the thrombin detection. *Anal. Chem.* **82**, 2341–6 (2010).
147. Swathi RS, Sebastiana KL. Resonance energy transfer from a dye molecule to graphene. *J. Chem. Phys.* **129**, 054703 (2008).
148. Heller DA, Baik S, Eurell TE, Strano MS. Single-walled carbon nanotube spectroscopy in live cells: Towards long-term labels and optical sensors. *Adv. Mater.* **17**, 2793–9 (2005).
149. Liu Z, Tabakman S, Welsher K, Dai H. Carbon nanotubes in biology and medicine: In vitro and in vivo detection, imaging and drug delivery. *Nano Res.* **1**, 85–120 (2009).
150. Leeuw TK, Reith RM, Simonette RA, Harden ME, Cherukuri P, Tsyboulski DA, Beckingham KM, Weisman RB. Single-walled carbon nanotubes in the intact organism: Near-IR imaging and biocompatibility studies in *Drosophila*. *Nano Lett.* **7**, 2650–4 (2007).
151. Keren S, Zavaleta C, Cheng Z, De La Zerda A, Gheysens O, Gambhir SS. Noninvasive molecular imaging of small living subjects using Raman spectroscopy. *Proc. Natl. Acad. Sci. USA* **105**, 5844–9 (2008).
152. Zavaleta C, De La Zerda A, Liu Z, Keren S, Cheng Z, Schipper M, Chen X, Dai H, Gambhir SS. Noninvasive Raman spectroscopy in living mice for evaluation of tumor targeting with carbon nanotubes. *Nano Lett.* **8**, 2800–5 (2008).
153. Xu MH, Wang LHV. Photoacoustic imaging in biomedicine. *Rev. Sci. Instrum.* **77**, 041101 (2006).
154. De La Zerda A, Zavaleta C, Keren S, Vaithilingam S, Bodapati S, Liu Z, Levi J, Ma T-J, Oralkan O, Cheng Z, et al. Photoacoustic molecular imaging in living mice utilizing targeted carbon nanotubes. *Nat. Nanotech.* **3**, 557–62 (2008).
155. Singh SK, Singh MK, Nayak MK, Kumari S, Grácio JJA, Dash D. Size distribution analysis and physical/fluorescence characterization of graphene oxide sheets by flow cytometry. *Carbon* **49**, 684 –92 (2011).

156. Prajapati VK, Awasthi K, Gautam S, Yadav TP, Rai M, Srivastava ON, Sundar S. Targeted killing of *Leishmania donovani* in vivo and in vitro with amphotericin B attached to functionalized carbon nanotubes. *J. Antimicrob. Chemother.* **66**, 874–9 (2011).
157. Schmidt ME, Blanton SA, Hines MA, Guyot-Sionnest P. Size-dependent two-photon excitation spectroscopy of CdSe nanocrystals. *Phys. Rev. B Condens. Matter* **53**, 12629–32 (1996).
158. Peng X, Manna L, Yang W, Wickham J, Scher E, Kadavanich A, Alivisatos AP. Shape control of CdSe nanocrystals. *Nature* **404**, 59–61 (2000).
159. Peng ZA, Peng X. Formation of high-quality CdTe, CdSe, and CdS nanocrystals using CdO as precursor. *J. Am. Chem. Soc.* **123**, 183–4 (2001).
160. Wilson WL, Szajowski PF, Brus LE. Quantum confinement in size-selected, surface-oxidized silicon nanocrystals. *Science* **262**, 1242–4 (1993).
161. Bruchez M Jr, Moronne M, Gin P, Weiss S, Alivisatos AP. Semiconductor nanocrystals as fluorescent biological labels. *Science* **28**, 2013–16 (1998).
162. Ekimov AI, Onushchenko AA. Quantum size effect in three-dimensional microscopic semiconductor crystals. *JETP Lett.* **34**, 345–9 (1981).
163. Service RF. Shortfalls in electron production dim hopes for MEG solar cells. *Science* **322**, 1784 (2008).
164. Bowers MJ, McBride JR, Rosenthal SJ. White-light emission from magic-sized cadmium selenide nanocrystals. *J. Am. Chem. Soc.* **127**, 15378–9 (2005).
165. Ledentsov NN. Quantum dot laser. *Semicond. Sci. Technol.* **26**, 014001 (2011).
166. Dahan M, Levi S, Luccardini C, Rostaing P, Riveau B, Triller A. Diffusion dynamics of glycine receptors revealed by single-quantum dot tracking. *Science* **302**, 442–5 (2003).
167. Norris DJ, Efros AL, Rosen M, Bawendi MG. Size dependence of exciton fine structure in CdSe quantum dots. *Phys. Rev. B Condens. Matter* **53**, 16347–54 (1996).
168. Medintz IL, Uyeda HT, Goldman ER, Mattoussi H. Quantum dot bioconjugates for imaging, labelling and sensing. *Nat. Mater.* **4**, 435–46 (2005).
169. Xing Y, Chaudry Q, Shen C, Kong KY, Zhau HE, Chung LW, Petros JA, O'Regan RM, Yezhelyev MV, Simons JW, Wang MD, Nie S. Bioconjugated quantum dots for multiplexed and quantitative immunohistochemistry. *Nat. Protoc.* **2**, 1152–65 (2007).
170. Murray CB, Norris DJ, Bawendi MG. Synthesis and characterization of nearly monodispersed CdE (E = S, Se, Te) semiconductor nanocrystallites. *J. Am. Chem. Soc.* **115**, 8706–15 (1993).
171. Yin Y, Xu X, Ge X, Lu Y, Zhang Z. Synthesis and characterization of ZnS colloidal particles via gamma-radiation. *Radiat. Phys. Chem.* **55**, 353–6 (1999).
172. Tsuji M, Hashimoto M, Nishizawa Y, Kubokawa M, Tsuji T. Microwave assisted synthesis of metallic nanostructures in solution. *Chem. Eur. J.* **11**, 440–52 (2005).
173. Corkery RW. Langmuir–Blodgett multilayer films. *Langmuir* **13**, 3591–4 (1997).
174. Feldmann C, Metzmacher C. Polyol mediated synthesis of nanoscale MS particles (M = Zn, Cd, Hg). *Mater. Chem.* **11**, 2603–6 (2001).
175. Lifshitz E, Dag I, Litvin I, Hodes G, Gorer S, Reisfeld R, Zelner M, Minti H. Optical properties of CdSe nanoparicels films prepared by chemical deposition and sol-gel methods. *Science* **288**, 188–96 (1998).
176. Liu YF, Yu JS. Selective synthesis of CdTe and high luminescence CdTe/CdS quantum dots: The effect of ligands. *J. Colloid Interface Sci.* **333**, 690–8 (2009).
177. Dabbousi B, Rodriguez-Viejo J, Mikulec F, Heine J, Mattoussi H, Ober R, et al. (CdSe)ZnS core-shell quantum dots: Synthesis and characterization of a size series of highly luminescent nanocrystallites. *J. Phys. Chem.* **101**, 9463–75 (1997).
178. Kang EC, Kataoka OK, Nagasaki Y. Preparation of water-soluble PEGylated semiconductor nanocrystals. *Chem. Lett.* **33**, 840–1 (2004).
179. Luccardini C, Tribet C, Vial F, Marchi-Artzner V, Dahan M. Size, charge, and interactions with giant lipid vesicles of quantum dots coated with an amphiphilic macromolecule. *Langmuir* **22**, 2304–10 (2006).
180. Wu XY, Liu H, Liu J, Haley KN, Treadway JA, Larson JP, Ge N, Peale F, Bruchez MP. Immunofluorescent labeling of cancer marker Her2 and other cellular targets with semiconductor QDs. *Nat. Biotechnol.* **21**, 41–6 (2003).
181. Chan WCW, Nie SM. Quantum dot bioconjugates for ultrasensitive nonisotopic detection. *Science* **281**, 2016–18 (1998).
182. Srinivasan C, Lee J, Papadimitrakopoulos F, Silbart LK, Zhao M, Burgess DJ. Labelling and intracellular tracking of functionally active plasmid DNA with semiconductor quantum dots. *Mol. Ther.* **14**, 192–201 (2006).
183. Koshman YE, Waters SB, Walker LA, Los T, de Tombe P, Goldspink PH, Russell B. Delivery and visualization of proteins conjugated to quantum dots in cardiac myocytes. *J. Mol. Cell Cardiol.* **45**, 853–6 (2008).
184. Wilson WL, Szajowski PF, Brus LE. Quantum confinement in size-selected, surface-oxidized silicon nanocrystals. *Science* **262**, 1242–4 (1993).
185. Xing Y, Chaudry Q, Shen C, Kong KY, Zhau HE, Chung LW, Petros JA, O'Regan RM, Yezhelyev MV, Simons JW, Wang MD, Nie S. Bioconjugated

quantum dots for multiplexed and quantitative immunohistochemistry. *Nat. Protoc.* **2**, 1152–65 (2007).
186. Shen J, Xu F, Jiang H, Wang Z, Tong J, Guo P, Ding S. Characterization and application of quantum dot nanocrystal monoclonal antibody conjugates for the determination of sulfamethazine in milk by fluoroimmunoassay. *Anal. Bioanal. Chem.* **389**, 2243–50 (2007).
187. Wu Y, Campos SK, Lopez GP, Ozbun MA, Sklar LA, Buranda T. The development of quantum dot calibration beads and quantitative multicolor bioassays in flow cytometry and microscopy. *Anal. Biochem.* **364**, 180–92 (2007).
188. Zahavy E, Freeman E, Lustig S, Keysary A, Yitzhaki S. Double labeling and simultaneous detection of B- and T cells using fluorescent nano-crystal (q-dots) in paraffin-embedded tissues. *J. Fluoresc.* **15**, 661–5 (2005).
189. Bostick RM, Kong KY, Ahearn TU, Chaudry Q, Cohen V, Wang MD. Detecting and quantifying biomarkers of risk for colorectal cancer using quantum dots and novel image analysis algorithms. *Conf. Proc. IEEE Eng. Med. Biol. Soc.* **1**, 3313–6 (2006).
190. Fountaine TJ, Wincovitch SM, Geho DH, Garfield SH, Pittaluga S. Multispectral imaging of clinically relevant cellular targets in tonsil and lymphoid tissue using semiconductor quantum dots. *Mod. Pathol.* **19**, 1181–91 (2006).
191. Sweeney E, Ward TH, Gray N, Womack C, Jayson G, Hughes A, Dive C, Byers R. Quantitative multiplexed quantum dot immunohistochemistry. *Biochem. Biophys. Res. Commun.* **374**, 181–6 (2008).
192. Schwock J, Ho JC, Luther E, Hedley DW, Geddie WR. Measurement of signaling pathway activities in solid tumor fine-needle biopsies by slide-based cytometry. *Diagn. Mol. Pathol.* **16**, 130–40 (2007).
193. Pathak S, Choi SK, Arnheim N, Thompson ME. Hydroxylated quantum dots as luminescent probes for in situ hybridization. *J. Am. Chem. Soc.* **123**, 4103–4 (2001).
194. Xiao Y, Barker PE. Semiconductor nanocrystal probes for human metaphase chromosomes. *Nucleic Acids Res.* **32**, e28 (2004).
195. Bentolila LA, Weiss S. Single-step multicolor fluorescence in situ hybridization using semiconductor quantum dot-DNA conjugates. *Cell Biochem. Biophys.* **45**, 59–70 (2006).
196. Ma L, Wu SM, Huang J, Ding Y, Pang DW, Li L. Fluorescence in situ hybridization (FISH) on maize metaphase chromosomes with quantum dot-labeled DNA conjugates. *Chromosoma* **117**, 181–7 (2008).
197. Wu SM, Zhao X, Zhang ZL, Xie HY, Tian ZQ, Peng J, Lu ZX, Pang DW, Xie ZX. Quantum-dot-labeled DNA probes for fluorescence in situ hybridization (FISH) in the microorganism *Escherichia coli*. *ChemPhysChem* **7**, 1062–7 (2006).
198. Matsuno A, Itoh J, Takekoshi S, Nagashima T, Osamura RY. Three-dimensional imaging of the intracellular localization of growth hormone and prolactin and their mRNA using nanocrystal (Quantum dot) and confocal laser scanning microscopy techniques. *J. Histochem. Cytochem.* **53**, 833–8 (2005).
199. Chan P, Yuen T, Ruf F, Gonzalez-Maeso J, Sealfon SC. Method for multiplex cellular detection of mRNAs using quantum dot fluorescent in situ hybridization. *Nucleic Acids Res.* **33**, e161 (2005).
200. Tholouli E, Hoyland JA, Di Vizio D, O'Connell F, Macdermott SA, Twomey D, Levenson R, Yin JA, Golub TR, Loda M, Byers R. Imaging of multiple mRNA targets using quantum dot based in situ hybridization and spectral deconvolution in clinical biopsies. *Biochem. Biophys. Res. Commun.* **348**, 628–36 (2006).
201. Choi Y, Kim HP, Hong SM, Ryu JY, Han SJ, Song R. In situ visualization of gene expression using polymer-coated quantum-dot-DNA conjugates. *Small* **5**, 2085–91 (2009).
202. Farkas DL, Du C, Fisher GW, Lau C, Niu W, Wachman ES, Levenson RM. Non-invasive image acquisition and advanced processing in optical bioimaging. *Comput. Med. Imaging Graph.* **22**, 89–102 (1998).
203. Gao X, Cui Y, Levenson RM, Chung LW, Nie S. In vivo cancer targeting and imaging with semiconductor quantum dots. *Nat. Biotechnol.* **22**, 969–76 (2004).
204. Lidke DS, Nagy P, Heintzmann R, Arndt-Jovin DJ, Post JN, Grecco HE, Jares-Erijman EA, Jovin TM. Quantum dot ligands provide new insights into erbB/HER receptor-mediated signal transduction. *Nat. Biotechnol.* **22**, 198–203 (2004).
205. Chen J, Pei Y, Chen Z, Cai J. Quantum dot labeling based on near-field optical imaging of CD44 molecules. *Micron* **41**, 198–202 (2010).
206. Gonda K,Watanabe TM, Ohuchi N, Higuchi H. In vivo nano-imaging of membrane dynamics in metastatic tumor cells using quantum dots. *J. Biol. Chem.* **285**, 2750–7 (2009).
207. Rieger S, Kulkarni RP, Darcy D, Fraser SE, Koster RW. Quantum dots are powerful multipurpose vital labelling agents in zebrafish embryos. *Dev. Dyn.* **234**, 670–81 (2005).
208. Voura EB, Jaiswal JK, Mattoussi H, Simon SM. Tracking metastatic tumor cell extravasation with quantum dot nanocrystals and fluorescence emission-scanning microscopy. *Nat. Med.* **10**, 993–8 (2004).

209. Slotkin JR, Chakrabarti L, Dai HN, Carney RS, Hirata T, Bregman BS, Gallicano GI, Corbin JG, Haydar TF. In vivo quantum dot labeling of mammalian stem and progenitor cells. *Dev. Dyn.* **236**, 3393–401 (2007).
210. Kobayashi H, Hama Y, Koyama Y, Barrett T, Regino CA, Urano Y, Choyke PL. Simultaneous multicolor imaging of five different lymphatic basins using quantum dots. *Nano Lett.* **7**, 1711–6 (2007).
211. Kim S, Lim YT, Soltesz EG, De Grand AM, Lee J, Nakayama A, Parker JA, Mihaljevic T, Laurence RG, Dor DM, Cohn LH, Bawendi MG, Frangioni JV. Near-infrared fluorescent type II quantum dots for sentinel lymph node mapping. *Nat. Biotechnol.* **22**, 93–7 (2004).
212. Soltesz EG, Kim S, Laurence RG, DeGrand AM, Parungo CP, Dor DM, Cohn LH, Bawendi MG, Frangioni JV, Mihaljevic T. Intraoperative sentinel lymph node mapping of the lung using near-infrared fluorescent quantum dots. *Ann. Thorac. Surg.* **79**, 269–77 (2005).
213. So MK, Xu C, Loening AM, Gambhir SS, Rao J. Self-illuminating quantum dot conjugates for in vivo imaging. *Nat. Biotechnol.* **24**, 339–43 (2006).
214. Zhang CY, Yeh HC, Kuroki MT, Wang TH. Single-quantum-dot-based DNA nanosensor. *Nat. Mater.* **4**, 826–31 (2005).
215. Yao H, Zhang Y, Xiao F, Xia ZY, Rao J. Quantum dot/bioluminescence resonance energy transfer based highly sensitive detection of proteases. *Angew. Chem. Int. Ed.* **46**, 4346–9 (2007).
216. Swain MD, Octain J, Benson DE. Unimolecular, soluble semiconductor nanoparticle-based biosensors for thrombin using charge/electron transfer. *Bioconjug. Chem.* **19**, 2520–6 (2008).
217. Jie G, Zhang J, Wang D, Cheng C, Chen HY, Zhu JJ. Electrochemiluminescence immunosensor based on CdSe nanocomposites. *Anal. Chem.* **80**, 4033–9 (2008).
218. Jiang H, Ju H. Enzyme–quantum dots architecture for highly sensitive electrochemiluminescence biosensing of oxidase substrates. *Chem. Commun.* **4**, 404–6 (2007).
219. Zhang CY, Johnson LW. Single quantum-dot-based aptameric nanosensor for cocaine. *Anal. Chem.* **81**, 3051–5 (2009).
220. Anas A, Akita H, Harashima H, Itoh T, Ishikawa M, Biju V. Photosensitized breakage and damage of DNA by CdSe–ZnS quantum dots. *J. Phys. Chem. B* **112**, 10005–11 (2008).
221. Juzenas P, Generalov R, Asta J, Juzeniene A, Moan J. Generation of nitrogen oxide and oxygen radicals by quantum dots. *J. Biomed. Nanotechnol.* **4**, 450–6 (2008).
222. Bagalkot V, Zhang L, Levy-Nissenbaum E, Jon S, Kantoff PW, Langer R, Farokhzad OC. Quantum dot–aptamer conjugates for synchronous cancer imaging, therapy, and sensing of drug delivery based on bi-fluorescence resonance energy transfer. *Nano Lett.* **7**, 3065–70 (2007).
223. Kakurai M, Demitsu T, Umemoto N, Ohtsuki M, Nakagawa H. Activation of mast cells by silver particles in a patient with localized argyria due to implantation of acupuncture needles. *Br. J. Dermatol.* **148**, 822 (2003).
224. Chaby G, Viseux V, Poulain JF, De Cagny B, Denoeux JP, Lok C. Topical silver sulfadiazine-induced acute renal failure. *Ann. Dermatol. Venereol.* **132**, 891–3 (2005).
225. Trop M. Silver-coated dressing acticoat caused raised liver enzymes and argyria-like symptoms in burn patient. *J. Trauma* **61**, 1024 (2006).
226. Sung JH, Ji JH, Yoon JU, Kim DS, Song MY, Jeong J, Han BS, Han JH, Chung YH, Kim J, et al. Lung function changes in Sprague-Dawley rats after prolonged inhalation exposure to silver nanoparticles. *Inhal. Toxicol.* **20**, 567–74 (2008).
227. Asharani PV, Wu YL, Gong Z, Valiyaveettil S. Toxicity of silver nanoparticles in zebrafish models. *Nanotechnology* **19**, 1–8 (2008).
228. Hsin YH, Chen CF, Huang S, Shih TS, Lai PS, Chueh PJ. The apoptotic effect of nanosilver is mediated by a ROS- and JNK-dependent mechanism involving the mitochondrial pathway in NIH3T3 cells. *Toxicol. Lett.* **179**, 130–9 (2008).
229. AshaRani PV, Mun GLK, Hande MP, Valiyaveettil S. Cytotoxicity and genotoxicity of silver nanoparticles in human cells. *ACS Nano* **3**, 279–90 (2009).
230. Stensberg MC, Wei Q, McLamore E, Porterfield DM, Wei A, Sepúlveda MS. Toxicological studies on silver nanoparticles: Challenges and opportunities in assessment, monitoring and imaging. *Nanomedicine (Lond.)* **6**, 879–98 (2011).
231. Chithrani BD, Ghazan AA, Chan CW. Determining the size and shape dependence of gold nanoparticle uptake into mammalian cells. *Nano Lett.* **6**, 662–8 (2006).
232. Patra HK, Banerjee S, Chaudhuri U, Lahiri P, Dasgupta AK. Cell selective response to gold nanoparticles. *Nanomedicine* **3**, 111–19 (2007).
233. Pan Y, Neuss S, Leifert A, Fischler M, Wen F, Simon U, Schmid G, Brandau W, Jahnen-Dechent W. Size-dependent cytotoxicity of gold nanoparticles. *Small* **3**, 1941–9 (2007).
234. Wang S, Lu W, Tovmachenko O, Rai US, Yu H, Ray PC. Challenge in understanding size and shape dependent toxicity of gold nanomaterials in human skin keratinocytes. *Chem. Phys. Lett.* **463**, 145–9 (2008).

235. Connor EE, Mwamuka J, Gole A, Murphy CJ, Wyatt MD. Gold nanoparticles are taken up by human cells but do not cause acute cytotoxicity. *Small* **1**, 325–7 (2005).
236. Shukla R, Bansal V, Chaudhary M, Basu A, Bhonde RR, Sastry M. Biocompatibility of gold nanoparticles and their endocytotic fate inside the cellular compartment: A microscopic overview. *Langmuir* **21**, 10644–54 (2005).
237. Goodman CM, McCusker CD, Yilmaz T, Rotello VM. Toxicity of gold nanoparticles functionalized with cationic and anionic side chains. *Bioconjug. Chem.* **15**, 897–900 (2004).
238. Alkilany AM, Murphy CJ. Toxicity and cellular uptake of gold nanoparticles: What we have learned so far? *J. Nanopart. Res.*, **12**, 2313–33 (2010).
239. Magrez A, Kasas S, Salicio V, Pasquier N, Seo JW, Celio M, Catsicas S, Schwaller B, Forró L. Cellular toxicity of carbon-based nanomaterials. *Nano Lett.* **6**, 1121–5 (2006).
240. Jia G, Wang H, Yan L, Wang X, Pei R, Yan T, Zhao Y, Guo X. Cytotoxicity of carbon nanomaterials: Single-wall nanotube, multi-wall nanotube, and fullerene. *Environ. Sci. Technol.* **39**, 1378–83 (2005).
241. Markovic Z, Trajkovic V. Biomedical potential of the reactive oxygen species generation and quenching by fullerenes (C60). *Biomaterials* **29**, 3561–73 (2008).
242. Shvedova AA, Fabisiak JP, Kisin ER, Murray AR, Roberts JR, Tyurina YY, Antonini JM, Feng WH, Kommineni C, Reynolds J, Barchowsky A, Castranova V, Kagan VE. Sequential exposure to carbon nanotubes and bacteria enhances pulmonary inflammation and infectivity. *Am. J. Respir. Cell Mol. Biol.* **38**, 579 (2008).
243. Muller J, Huaux F, Moreau N, Misson P, Heilier JF, Delos M. Respiratory toxicity of multi-wall carbon nanotubes. *Toxicol. Appl. Pharmacol.* **207**, 221 (2005).
244. Radomski A, Jurasz P, Alonso-Escolano D, Drews M, Morandi M, Malinski T, Radomski MW. Nanoparticle-induced platelet aggregation and vascular thrombosis. *Br. J. Pharmacol.* **146**, 882–93 (2005).
245. Manna SK, Sarkar S, Barr J, Wise K, Barrera EV, Jejelowo O, Rice-Ficht AC, Ramesh GT. Single-walled carbon nanotube induces oxidative stress and activates nuclear transcription factor-kappaB in human keratinocytes. *Nano Lett.* **5**, 1676 (2005).
246. Nerl HC, Cheng C, Goode AE, Bergin SD, Lich B, Gass M, Porter AE. Imaging methods for determining uptake and toxicity of carbon nanotubes in vitro and in vivo. *Nanomedicine (Lond.)* **6**, 849–65 (2011).
247. Bihari P, Holzer M, Praetner M, Fent J, Lerchenberger M, Reichel CA, Rehberg M, Lakatos S, Krombach F. Single-walled carbon nanotubes activate platelets and accelerate thrombus formation in the microcirculation. *Toxicology* **269**, 148 (2010).
248. Semberova J, Lacerda SHDP, Simakova O, Holada K, Gelderman MP, Simak J. Carbon nanotubes activate blood platelets by inducing extracellular Ca^{2+} influx sensitive to calcium entry inhibitors. *Nano Lett.* **9**, 3312 (2009).
249. Saller F, Schapira M, Angelillo-Scherrer A. Role of platelet signaling in thrombus stabilization: Potential therapeutic implications. *Curr. Signal Transduct. Ther.* **3**, 22–54 (2008).
250. Badruddin A, Gorelick PB. Antiplatelet therapy for prevention of recurrent stroke. *Curr. Treat. Options Neurol.* **11**, 452–9 (2009).
251. Talavera YA, Hernandez IM, Portilla CV. Platelet activation: Basic aspects, its role in cerebrovascular disease and its therapeutic projections. *Revista Ecuatoriana Neurologia* **16**, 127 (2007).
252. Chang Y, Yanga ST, Liua JH, Dong E, Wang Y, Cao A, Liu Y, Wang H. In vitro toxicity evaluation of graphene oxide on A549 cells. *Toxicol. Lett.* **200**, 201 (2011).
253. Zhang Y, Ali SF, Dervishi E, Xu Y, Li Z, Casciano D, Biris AS. Cytotoxicity effects of graphene and single-wall carbon nanotubes in neural phaeochromocytoma-derived PC12 cells. *ACS Nano* **4**, 3181 (2010).
254. Agarwal S, Zhou X, Ye F, He Q, Chen GCK, Soo J, Beoy F, Zhang H, Chen P. Interfacing live cells with nanocarbon substrates. *Langmuir* **26**, 2244 (2010).
255. Wang K, Ruan J, Song H, Zhang J, Wo Y, Guo S, Cui D. Biocompatibility of graphene oxide. *Nanoscale Res. Lett* **6**, 8 (2011).
256. Sasidharan A, Panchakarla LS, Chandran P, Menon D, Nair S, Rao CNR, Koyakutty M. Differential nano-bio interactions and toxicity effects of pristine *versus* functionalized grapheme. *Nanoscale* **3**, 2461–4 (2011).
257. Singh SK, Singh MK, Nayak MK, Kumari S, Shrivastava S, Gracio JA, Dash D. Thrombus inducing property of atomically thin graphene oxide sheets. *ACS Nano* **5**, 4987–96 (2011).
258. Bertin G, Averbeck D. Cadmium: Cellular effects, modifications of biomolecules, modulation of DNA repair and genotoxic consequences (a review). *Biochimie* **88**, 1549–59 (2006).
259. Taylor A. Biochemistry of tellurium. *Biol. Trace Elem. Res.* **55**, 231–9 (1996).
260. Vinceti M, Wei ET, Malagoli C, Bergomi M, Vivoli G. Adverse health effects of selenium in humans. *Rev. Environ. Health* **16**, 233–51 (2001).
261. Dubertret B, Skourides P, Norris D, Noireaux V, Brivanlou A, Libchaber A. In vivo imaging of quantum dots encapsulated in phospholipid micelles. *Science* **298**, 1759–62 (2002).
262. Noh YW, Lim YT, Chung BH. Noninvasive imaging of dendritic cell migration into lymph nodes using

near-infrared fluorescent semiconductor nanocrystals. *FASEB J.* **22**, 3908–18 (2008).
263. Ohyabu Y, Kaul Z, Yoshioka T, Inoue K, Sakai S, Mishima H, Uemura T, Kaul SC, Wadhwa R. Stable and non-disruptive in vitro/in vivo labeling of mesenchymal stem cells by internalizing quantum dots. *Hum. Gene Ther.* **20**, 217–24 (2009).
264. Akerman M, Chan W, Laakkonen P, Bhatia S, Ruoslahti E. Nanocrystal targeting in vivo. *Proc. Natl. Acad. Sci. USA* **99**, 12617–21 (2002).
265. Lee HM, Shin DM, Song HM, Yuk JM, Lee ZW, Lee SH, Hwang SM, Kim JM, Lee CS, Jo EK. Nanoparticles up-regulate tumor necrosis factor-alpha and CXCL8 via reactive oxygen species and mitogen-activated protein kinase activation. *Toxicol. Appl. Pharmacol.* **238**, 160–9 (2009).
266. Stern ST, Zolnik BS, McLeland CB, Clogston J, Zheng J, McNeil SE. Induction of autophagy in porcine kidney cells by quantum dots: A common cellular response to nanomaterials? *Toxicol. Sci.* **106**, 140–52 (2008).
267. Derfus A, Chan W, Bhatia S. Probing the cytotoxicity of semiconductor quantum dots. *Nano Lett.* **4**, 11–18 (2004).
268. Hoshino A, Fujioka K, Oku T, Suga M, Sasaki Y, Ohta T, et al. Physicochemical properties and cellular toxicity of nanocrystal quantum dots depend on their surface modification. *Nano Lett.* **4**, 2163–9 (2004).
269. Lovric J, Bazzi H, Cuie Y, Fortin G, Winnik F, Maysinger D. Differences in subcellular distribution and toxicity of green and red emitting CdTe quantum dots. *J. Mol. Med.* **83**, 377–85 (2005).
270. Warner JH, Hoshino A, Yamamoto K, Tilley RD. Water-soluble photoluminescent silicon quantum dots. *Angew. Chem. Int. Ed. Engl.* **44**, 4550–4 (2005).
271. Botsoa J, Lysenko V, Géloën A, Marty O, Bluet J, Guillot G. Application of 3C-SiC quantum dots for living cell imaging. *Appl. Phys. Lett.* **92**, 173902–3 (2008).
272. Qian J, Yong KT, Roy I, Ohulchanskyy TY, Bergey EJ, Lee HH, Tramposch KM, He S, Maitra A, Prasad PN. Imaging pancreatic cancer using surface-functionalized quantum dots. *J. Phys. Chem. B* **111**, 6969–72 (2007).
273. Mahler B, Spinicelli P, Buil S, Quelin X, Hermier JP, Dubertret B. Towards non-blinking colloidal quantum dots. *Nat. Mater.* **7**, 659–64 (2008).
274. Shi Y, He P, Zhu X. Photoluminescence-enhanced biocompatible quantum dots by phospholipid functionalization. *Mater. Res. Bull.* **43**, 2626–35 (2008).